Table 2. Area Under the ROC Curves, Sensitivity, Specificity, and Negative as Well as Positive Predictive Values of Nonvirological Responses

Variables	AUC	95% CI	Cutoff	Sensitivity	Specificity	NPV	PPV
RIG-I (copies/int. control)	0.712	0.584-0.840	0.573	0.679	0.733	0.830	0.543
ISG15 (copies/int. control)	0.782	0.666-0.899	0.347	0.714	0.833	0.862	0.667
RIG-I/IPS-1 (copies/int. control)	0.732	0.611-0.852	0.651	0.679	0.750	0.833	0.559
IL28B genotype	0.662	0.537-0.787	TG*/CT†	0.607	0.717	0.796	0.500

AUC, area under the curve; NPV, negative predictive value; PPV, positive predictive value.
*Genotype at rs8099917.
†Genotype at rs12979860.

associated with NVR (Table 3). Among these, multivariate analysis identified old age, HCV core double mutant, and higher hepatic expressions of *RIG-I* and *ISG15* as factors independently associated with NVR (Table 3).

IPS-1 and RIG-I Protein Expression in the Liver. Western blotting revealed that full-length and cleaved IPS-1 were variably present in all the samples from CH-C patients (Fig. 5A). Similar to mRNA

Table 3. Factors Associated with Nonvirological Response

	Univariate Analysis		Multivariate Analysis*	
Factors	Risk Ratio (95% CI)	*P*-value	Risk Ratio (95% CI)	*P*-value
Age (by every 10 year)	1.84 (1.10-3.14)	0.027	3.76 (1.19-11.7)	0.023
Sex				
Male	1			
Female	1.62 (0.59-4.42)	0.350		
BMI (by every 5 kg/m^2)	0.87 (0.46-1.65)	0.672		
Fibrosis stage				
F1/F2	1			
F3/F4	1.82 (0.69-4.85)	0.228		
Degree of steatosis				
<10%	1			
≥10%	1.46 (0.43-5.03)	0.544		
Albumin (by every 1 g/dL)	0.41 (0.11-1.56)	0.190		
AST (by every 40 IU/L)	0.89 (0.53-1.56)	0.681		
ALT (by every 40 IU/L)	0.85 (0.57-1.32)	0.481		
γ-GTP (by every 40 IU/L)	1.32 (0.82-2.07)	0.235		
Fasting blood sugar (by every 100 mg/dL)	1.35 (0.74-2.45)	0.340		
Hemoglobin (by every 1 g/dL)	0.93 (0.67-1.31)	0.683		
Platelet counts (by every 10^4/μL)	0.90 (0.82-0.99)	0.037	0.92 (0.78-1.08)	0.296
HCV load (by every 100 KIU/mL)	1.00 (1.00-1.00)	0.688		
Core 70 & 91 double mutation				
Wild	1		1	
Mutant	3.92 (1.14-13.5)	0.030	11.1 (1.40-88.7)	0.023
ISDR				
Nonwildtype	1			
Wildtype	1.38 (0.13-3.61)	0.513		
IL28B genotype				
Major allele†	1		1	
Minor allele‡	3.91 (1.52-10.0)	0.005	1.53 (0.20-11.9)	0.684
Hepatic gene expression (by every 0.1 copy/*int. control*)				
RIG-I	1.28 (1.10-1.50)	0.002	1.53 (1.07-2.22)	0.021
MDA5	1.53 (1.12-2.00)	0.001		
LGP2	1.34 (1.04-1.74)	0.026		
IPS-1	0.90 (0.78-1.04)	0.143		
RNF125	0.93 (0.83-1.04)	0.204		
ISG15	1.37 (1.16-1.62)	<0.001	1.28 (1.04-1.58)	0.021
USP18	1.67 (1.27-2.20)	<0.001		
IFNλ	1.02 (0.99-1.05)	0.170		
RIG-I/IPS-1 ratio (by every 0.1)	1.21 (1.07-1.36)	0.002		

Risk ratios for nonvirological response were calculated by the logistic regression analysis. BMI, body mass index; AST, aspartate aminotransferase; ALT, alanine aminotransferase; γ-GTP, gamma-glutamyl transpeptidase; HCV, hepatitis C virus; ISDR, IFN sensitivity determining region.
*Multivariate analysis was performed with factors significantly associated with nonvirological response by univariate analysis except for *MDA5*, *LGP2*, *USP18*, and *RIG-I/IPS-1* ratio, which were significantly correlated with *RIG-I* and *ISG15*.
†rs8099917 TT and rs12979860 CC.
‡rs8099917 TG and rs12979860 CT.

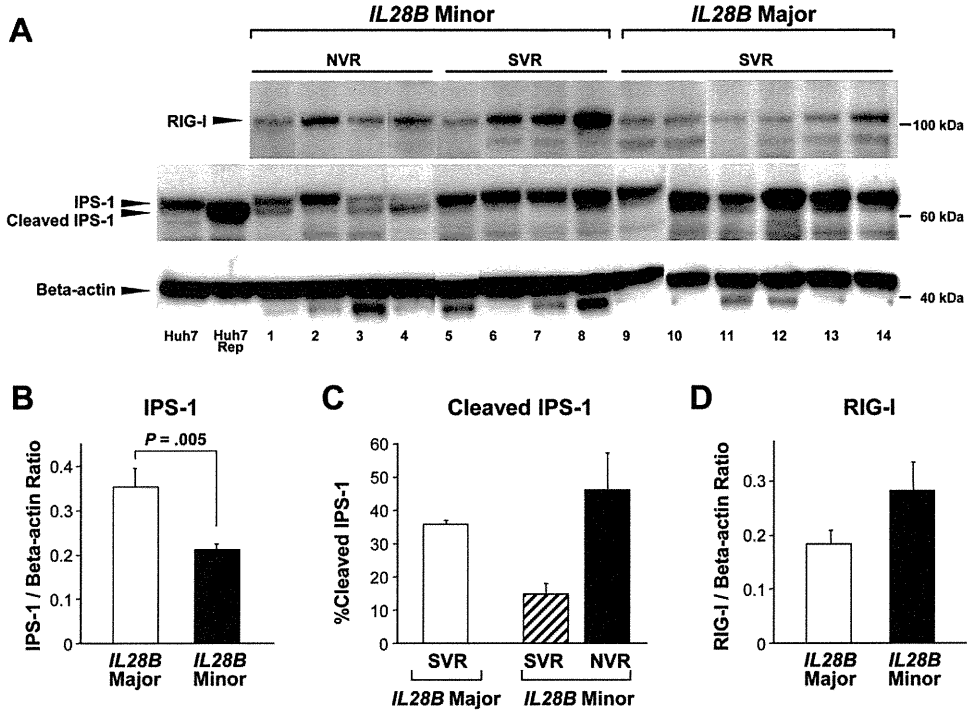

Fig. 5. (A) Western blotting for IPS-1 and RIG-I protein expression levels. Eight lanes contain samples from *IL28B* minor patients (lanes 1-8) and six lanes contain samples from *IL28B* major patients (lanes 9-14). Four lanes contain samples from nonvirological responders (NVR, lanes 1-4) and 10 lanes contain samples from sustained virological responders (SVR, lanes 5-14). Specific bands for RIG-I, full-length IPS-1, cleaved IPS-1, and β-actin are indicated by arrows. Naive Huh7 cells were used for a positive control for full-length IPS-1 (lane Huh7), and cells transfected with HCV-1b subgenomic replicon (Reference #20) were used for a positive control for cleaved IPS-1 (lane Huh7 Rep). (B) Total IPS-1 protein expression levels normalized to β-actin according to *IL28B* genotype. Error bars indicate standard error. *P*-value was determined by Mann-Whitney *U* test. (C) Percentage of cleaved IPS-1 products in total IPS-1 protein according to treatment responses stratified by *IL28B* genotype. Error bars indicate standard error. (D) RIG-I protein expression levels normalized to β-actin according to *IL28B* genotype. Error bars indicate standard error.

expression, total hepatic IPS-1 protein expression was significantly lower in *IL28B* minor patients than in *IL28B* major patients (Fig. 5B). With regard to *IL28B* minor patients, the percentage of cleaved IPS-1 protein in total IPS-1 in SVR was lower than that in NVR (Fig. 5C). In contrast to IPS-1 protein expression, hepatic RIG-I protein expression was higher in *IL28B* minor patients than that in *IL28B* major patients (Fig. 5D).

Discussion

In the present study we found that the baseline expression levels of intrahepatic viral sensors and related regulatory molecules were significantly associated with the genetic variation of *IL28B* and final virological outcome in CH-C patients treated with PEG-IFNα/RBV combination therapy. Although the relationship between the *IL28B* minor allele and NVR in PEG-IFNα/RBV combination therapy is evident, mechanisms responsible for this association remain unknown. *In vitro* studies have suggested that cytoplasmic viral sensors, such as RIG-I and MDA5, play a pivotal role in the regulation of IFN production and augment IFN production through an amplification circuit.[7,8] Our results indicate that expressions of *RIG-I* and *MDA5* and a related amplification system may be up-regulated by endogenous IFN at a higher baseline level in *IL28B* minor patients. However, HCV elimination by subsequent exogenous IFN is insufficient in these patients, as reported,[19] suggesting that *IL28B* minor patients may have adopted a different equilibrium in their innate immune response to HCV. Our data are further supported by recent reports of an association between intrahepatic levels of IFN-stimulated gene expression and PEG-IFNα/RBV response as well as with *IL28B* genotype.[21-23]

In contrast to cytoplasmic viral sensor (*RIG-I, MDA5*, and *LGP2*) and modulator (*ISG15* and *USP18*) expression, the adaptor molecule (*IPS-1*) expression was significantly lower in *IL28B* minor patients. Moreover, western blotting further confirmed IPS-1 protein downregulation in *IL28B* minor patients by revealing decreased protein levels. Because IPS-1 is one of the main target molecules of HCV evasion,[9,18]

transcriptional and translational *IPS-1* expression are probably suppressed by HCV with resistant phenotype, which may be more adaptive in *IL28B* minor patients than in *IL28B* major patients. When we analyzed the proportion of full-length or cleaved IPS-1 to the total IPS-1 protein in a subgroup of *IL28B* minor patients, cleaved IPS-1 product was less dominant in SVR than in NVR, whereas uncleaved full-length IPS-1 protein was more dominant in SVR than in NVR. Therefore, the ability of HCV to evade host innate immunity by cleaving IPS-1 protein and/or host capability of protection from IPS-1 cleavage is probably responsible for the variable treatment responses in *IL28B* minor patients.

Our results indicated a close association between *IL28B* minor patients with higher γ-GTP level and higher frequency of HCV core double mutants, which are known factors for NVR. In contrast, no significant association was observed between *IL28B* genotype and age, gender, or liver fibrosis, which are also known to be unfavorable factors for virological response to PEG-IFNα/RBV. Therefore, certain factors other than the *IL28B* genotype may independently influence virological response. To elucidate whether gene expression involving innate immunity independently associates with a virological response from the *IL28B* genotype, we performed further analysis in a subgroup and conducted a multivariate regression and ROC analyses. Our multivariate and ROC analyses demonstrate that higher expressions of *RIG-I* and *ISG15* as well as a higher ratio of *RIG-I/IPS-1* are independently associated with NVR, and quantification of these values is more useful in predicting final virological response to PEG-IFNα/RBV than determination of *IL28B* genotype in each individual patients. However, the SVR rates in our patients were similar among *IL28B* genotypes, which suggests more SVR patients with the *IL28B* minor allele were included in the present study than those in the general CH-C population. Hence, our data did not necessarily exclude the possibility of the *IL28B* genotype in predicting NVR, although our multivariate analysis could not identify the *IL28B* minor allele as an independent factor for NVR. Interestingly, an association between *IL28B* genotype and expressions of *RIG-I* and *ISG15* as well as *RIG-I/IPS-1* expression ratio is still observed even in patients with the same subgroup of virological response (Fig. 3).

In the present study, although hepatic *IFNλ* expression was observed to be higher in *IL28B* minor and NVR patients, it was not statistically significant. Because *IL28B* shares 98.2% homology with *IL28A*, our primer could not distinguish the expression of *IL28B* from that of *IL28A*, and moreover, we could not specify which cell expresses *IFNλ* (i.e., hepatocytes or other immune cells that have infiltrated the liver). Therefore, the precise mechanisms underlying *IL28B* variation and expression of *IFNλ* in relation to treatment response need further clarification by specifying type of IFNλ and uncovering the producing cells.

In the present study we included genotype 1b patients because it is imperative to designate a virologically homogenous patient group to associate individual treatment responses with different gene expression profiles that direct innate immune responses. We have reported that the *RIG-I/IPS-1* ratio was significantly higher in NVR with HCV genotype 2.[19] However, our preliminary results indicated that baseline hepatic *RIG-I* and *ISG15* expression and the *RIG-I/IPS-1* expression ratio is not significantly different among *IL28B* genotypes in patients infected with genotype 2 (Supporting Figure). This may be related to the rarity of NVR with HCV genotype 2 and the lower effect of *IL28B* genotype on virological responses in patients infected with HCV genotype 2.[24] The association among treatment responses in all genotypes, the different status of innate immune responses, and *IL28B* genotype needs to be examined further.

Differences in allele frequency for *IL28B* SNPs among the population groups has been reported. The frequency of *IL28B* major allele among patients with Asian ancestry is higher than that among patients with European and African ancestry.[25] Because *IL28B* polymorphism strongly influences treatment responses within each population group,[5] our data obtained from Japanese patients can be applied to other population groups. However, the rate of SVR having African ancestry was lower than that having European ancestry within the same *IL28B* genotype.[5] Hence, further study is required to clarify whether this difference among the population groups with the same *IL28B* genotype could be explained by differences in expression of genes involved in innate immunity.

In a recent report, an SVR rate of telaprevir with PEG-IFNα/RBV was only 27.6% in *IL28B* minor patients.[26] Because new anti-HCV therapy should still contain PEG-IFNα/RBV as a platform for the therapy, our findings regarding innate immunity in addressing the mechanism of virological response and predicting NVR remain important in this new era of directly acting anti-HCV agents, such as telaprevir and boceprevir.

In conclusion, this clinical study in humans demonstrates the potential relevance of the molecules involved in innate immunity to the genetic variation

of *IL28B* and clinical response to PEG-IFNα/RBV. Both the *IL28B* minor allele and higher expressions of *RIG-I* and *ISG15* as well as higher *RIG-I/IPS-1* ratio are independently associated with NVR. Innate immune responses in *IL28B* minor patients may have adapted to a different equilibrium compared with that in *IL28B* major patients. Our data will advance both understanding of the pathogenesis of HCV resistance and the development of new antiviral therapy targeted toward the innate immune system.

References

1. Kiyosawa K, Sodeyama T, Tanaka E, Gibo Y, Yoshizawa K, Nakano Y, et al. Interrelationship of blood transfusion, non-A, non-B hepatitis and hepatocellular carcinoma: analysis by detection of antibody to hepatitis C virus. HEPATOLOGY 1990;12:671-675.
2. Zeuzem S, Pawlotsky JM, Lukasiewicz E, von Wagner M, Goulis I, Lurie Y, et al. DITTO-HCV Study Group. International, multicenter, randomized, controlled study comparing dynamically individualized versus standard treatment in patients with chronic hepatitis C. J Hepatol 2005;43:250-257.
3. Tanaka Y, Nishida N, Sugiyama M, Kurosaki M, Matsuura K, Sakamoto N, et al. Genome-wide association of IL28B with response to pegylated IFN-alpha and ribavirin therapy for chronic hepatitis C. Nat Genet 2009;10:1105-1109.
4. Suppiah V, Moldovan M, Ahlenstiel G, Berg T, Weltman M, Abate ML, et al. IL28B is associated with response to chronic hepatitis C IFN-alpha and ribavirin therapy. Nat Genet 2009;10:1100-1104.
5. Ge D, Fellay J, Thompson AJ, Simon JS, Shianna KV, Urban TJ, et al. Genetic variation in IL28B predicts hepatitis C treatment-induced viral clearance. Nature 2009;461:399-401.
6. Biron CA. Initial and innate responses to viral infections—pattern setting in immunity or disease. Curr Opin Microbiol 1999;2:374-381.
7. Yoneyama M, Kikuchi M, Natsukawa T, Shinobu N, Imaizumi T, Miyagishi M, et al. The RNA helicase RIG-I has an essential function in double-stranded RNA-induced innate antiviral responses. Nat Immunol 2004;5:730-737.
8. Yoneyama M, Kikuchi M, Matsumoto K, Imaizumi T, Miyagishi M, Taira K, et al. Shared and unique functions of the DExD/H-box helicases RIG-I, MDA5, and LGP2 in antiviral innate immunity. J Immunol 2005;175:2851-2858.
9. Meylan E, Curran J, Hofmann K, Moradpour D, Binder M, Bartenschlager R, et al. Cardif is an adaptor protein in the RIG-I antiviral pathway and is targeted by hepatitis C virus. Nature 2005;437:1167-1172.
10. Kawai T, Takahashi K, Sato S, Coban C, Kumar H, Kato H, et al. IPS-1, an adaptor triggering RIG-I- and Mda5-mediated type I interferon induction. Nat Immunol 2005;6:981-988.
11. Seth RB, Sun L, Ea CK, Chen ZJ. Identification and characterization of MAVS, a mitochondrial antiviral signaling protein that activates NF-kappaB and IRF 3. Cell 2005;122:669-682.
12. Xu LG, Wang YY, Han KJ, Li LY, Zhai Z, Shu HB. VISA is an adapter protein required for virus-triggered IFN-beta signaling. Mol Cell 2005;19:727-740.
13. Rothenfusser S, Goutagny N, DiPerna G, Gong M, Monks BG, Schoenemeyer A, et al. The RNA helicase Lgp2 inhibits TLR-independent sensing of viral replication by retinoic acid-inducible gene-I. J Immunol 2005;175:5260-5268.
14. Arimoto K, Takahashi H, Hishiki T, Konishi H, Fujita T, Shimotohno K. Negative regulation of the RIG-I signaling by the ubiquitin ligase RNF125. Proc Natl Acad Sci U S A 2007;104:7500-7505.
15. Zhao C, Denison C, Huibregtse JM, Gygi S, Krug RM. Human ISG15 conjugation targets both IFN-induced and constitutively expressed proteins functioning in diverse cellular pathways. Proc Natl Acad Sci U S A 2005;102:10200-10205.
16. Schwer H, Liu LQ, Zhou L, Little MT, Pan Z, Hetherington CJ, et al. Cloning and characterization of a novel human ubiquitin-specific protease, a homologue of murine UBP43 (Usp18). Genomics 2000;65:44-52.
17. Malakhov MP, Malakhova OA, Kim KI, Ritchie KJ, Zhang DE. UBP43 (USP18) specifically removes ISG15 from conjugated proteins. J Biol Chem 2002;277:9976-9981.
18. Li XD, Sun L, Seth RB, Pineda G, Chen ZJ. Hepatitis C virus protease NS3/4A cleaves mitochondrial antiviral signaling protein off the mitochondria to evade innate immunity. Proc Natl Acad Sci U S A 2005;102:17717-17722.
19. Asahina Y, Izumi N, Hirayama I, Tanaka T, Sato M, Yasui Y, et al. Potential relevance of cytoplasmic viral sensors and related regulators involving innate immunity in antiviral response. Gastroenterology 2008;134:1396-1405.
20. Tanabe Y, Sakamoto N, Enomoto N, Kurosaki M, Ueda E, Maekawa S, et al. Synergistic inhibition of intracellular hepatitis C virus replication by combination of ribavirin and interferon-alpha. J Infect Dis 2004;189:1129-1139.
21. Honda M, Sakai A, Yamashita T, Nakamoto Y, Mizukoshi E, Sakai Y, et al. Hepatic ISG expression is associated with genetic variation in interleukin 28B and the outcome of IFN therapy for chronic hepatitis C. Gastroenterology 2010;139:499-509.
22. Urban TJ, Thompson AJ, Bradric SS, Fellay J, Schuppan D, Cronin KD, et al. *IL28B* genotype is associated with differential expression of intrahepatic interferon-stimulated genes in patients with chronic hepatitis C. HEPATOLOGY 2010;52:1888-1896.
23. Dill MT, Duong FHT, Vogt JE, Bibert S, Bochud PY, Terracciano L, et al. Interferon-induced gene expression is a stronger predictor of treatment response than *IL28B* genotype in patients with hepatitis C. Gastroenterology 2011;140:1021-1031.
24. Yu ML, Huang CF, Huang JF, Chang NC, Yang JF, Lin ZY, et al. Role of interleukin-28B polymorphism in the treatment of hepatitis C virus genotype 2 infection in Asian patients. HEPATOLOGY 2011;53:7-13.
25. Thomas DL, Thio CL, Martin MP, Qi Y, Ge D, O'hUigin C, Kidd J, et al. Genetic variation in *IL28B* and spontaneous clearance of hepatitis C virus. Nature 2009;461:798-802.
26. Akuta N, Suzuki F, Hirakawa M, Kawamura Y, Yatsuji H, Sezaki H, et al. Amino acid substitution in hepatitis C virus core region and genetic variation near the interleukin 28B gene predict viral response to teraprevir with pegIFN and ribavirin. HEPATOLOGY 2010;52:421-429.

Cell. Mol. Life Sci.
DOI 10.1007/s00018-012-0940-6

Cellular and Molecular Life Sciences

RESEARCH ARTICLE

Let-7b is a novel regulator of hepatitis C virus replication

Ju-Chien Cheng · Yung-Ju Yeh · Ching-Ping Tseng · Sheng-Da Hsu · Yu-Ling Chang · Naoya Sakamoto · Hsien-Da Huang

Received: 29 September 2011 / Revised: 28 January 2012 / Accepted: 9 February 2012

Abstract The non-coding microRNA (miRNA) is involved in the regulation of hepatitis C virus (HCV) infection and offers an alternative target for developing anti-HCV agent. In this study, we aim to identify novel cellular miRNAs that directly target the HCV genome with anti-HCV therapeutic potential. Bioinformatic analyses were performed to unveil liver-abundant miRNAs with predicted target sequences on HCV genome. Various cell-based systems confirmed that let-7b plays a negative role in HCV expression. In particular, let-7b suppressed HCV replicon activity and down-regulated HCV accumulation leading to reduced infectivity of HCVcc. Mutational analysis identified let-7b binding sites at the coding sequences of NS5B and 5′-UTR of HCV genome that were conserved among various HCV genotypes. We further demonstrated that the underlying mechanism for let-7b-mediated suppression of HCV RNA accumulation was not dependent on inhibition of HCV translation. Let-7b and IFNα-2a also elicited a synergistic inhibitory effect on HCV infection. Together, let-7b represents a novel cellular miRNA that targets the HCV genome and elicits anti-HCV activity. This study thereby sheds new insight into understanding the role of host miRNAs in HCV pathogenesis and to developing a potential anti-HCV therapeutic strategy.

Keywords microRNA · Let-7b · HCV

Ju-Chien Cheng and Yung-Ju Yeh contributed equally to this work.

Electronic supplementary material The online version of this article (doi:10.1007/s00018-012-0940-6) contains supplementary material, which is available to authorized users.

J.-C. Cheng (✉) · Y.-J. Yeh · Y.-L. Chang
Department of Medical Laboratory Science and Biotechnology, China Medical University, Taichung 404, Taiwan, ROC
e-mail: jccheng@mail.cmu.edu.tw

C.-P. Tseng
Department of Medical Biotechnology and Laboratory Science, Chang Gung University, Taoyuan, Taiwan, ROC

Y.-J. Yeh · S.-D. Hsu · H.-D. Huang (✉)
Institute of Bioinformatics and Systems Biology, National Chiao Tung University, Hsinchu 300, Taiwan, ROC
e-mail: bryan@mail.nctu.edu.tw

N. Sakamoto
Department of Gastroenterology and Hepatology, Tokyo Medical and Dental University, Tokyo, Japan

H.-D. Huang
Department of Biological Science and Technology, National Chiao Tung University, Hsinchu 300, Taiwan, ROC

Abbreviations

miRNA	microRNA
HCV	Hepatitis C virus
MRE	MicroRNA responsive element
IFNα-2a	Peginterferon alpha-2a
IFN	Interferon
LF2000	Lipofectamine 2000
DMEM	Dulbecco's modified Eagle's medium
FITC	Fluorescein isothiocyanate
DAPI	4′,6-diamidino-2-phenylindole

Introduction

Hepatitis C virus (HCV) frequently causes chronic infection, leading to hepatic fibrosis and hepatocellular carcinoma [1]. Due to the lack of viral vaccine, the population affected by HCV infection is increased substantially [2]. With the strong side-effects and the moderate successful rate associated with the first-line interferon (IFN)-based

Published online: 06 March 2012

treatment [3], development of effective therapeutic regimens is still an emerging focus in the control of HCV infection.

Small molecules such as telaprevir have been developed to alleviate disease progression. However, the infidelity of HCV RNA polymerase constantly causes mutation and genome instability that result in the generation of drug-resistant viral strain [4, 5]. Targeting the host factors with important roles in viral infection offers an alternative strategy for development of anti-HCV regimen [6]. Apart from host proteins, a new class of small non-coding endogenous RNA molecule microRNA (miRNA) has been recently unveiled [7]. Although it is not yet fully clarified, miRNA is involved in various biological functions, including the response to HCV infection [7–10]. For example, miR-122 enhances whereas mir-199a* suppresses HCV replication and viral production [11–13]; interferon β (IFN-β)-mediated attenuation of viral replication is associated with an increase in miRNAs that have predicted target sequences within the HCV genome [14]. In addition, miRNA effectors including Argonaute 2 (Ago2) and DDX6 were found to positively regulate HCV replication [15, 16]. These findings suggest that cellular miRNAs regulate HCV gene expression and play roles in the host response against HCV infection.

In this study, bioinformatic analyses were performed to identify liver miRNAs targeting the HCV genome. Various cellular and viral systems were used to confirm bioinformatic prediction and to investigate the functional effects of the selected miRNAs. Our data reveal for the first time that let-7b is a negative regulator of HCV replication with the effective target sequences located on the 5′-untranslation region (UTR) and NS5B coding region of the HCV genome. The suppressive effect of let-7b on HCV RNA is not through translation inhibition. Besides, let-7b and Peginterferon alpha-2a (IFNα-2a) elicit a synergistic inhibitory effect on HCV infection. The roles of let-7b in the regulation of HCV pathogenesis and in the development of novel anti-HCV therapeutic strategy are discussed.

Materials and methods

Materials

The plasmid pRep-Feo and the replicon cells Huh7/Rep-Feo were obtained from Dr. Naoya Sakamoto (Tokyo Medical and Dental University). The plasmids pFL-J6/JFH, pJ6/JFH(p7-Rlu2A), and pJ6/JFH(p7-Rlu2A)GNN, the ConI replicon cells and Huh7.5 [17, 18], were kindly provided by Professor Charles Rice (The Rockefeller University, NY). The plasmid JC1-Luc2A, which replaced the Rluc gene of pJ6/JFH(p7-Rlu2A) to firefly luciferase (Luc) gene was kindly provided by Professor Robert T. Schooley (University of California San Diego, CA). Pre-miRNA, miRNA inhibitors and negative control for miRNA and miRNA inhibitors were purchased from Ambion (Austin, TX). The pLKO.1-shGFP control plasmid (clone ID: TRCN0000072197) and the two pLKO.1-shHMGA2 plasmids (clone ID: TRCN0000021965 and TRCN0000021968) were purchased from National RNAi Core Facility (Academia Sinica, Taiwan). The Lipofectamine 2000 (LF2000) and RNAiMAX transfection reagents were purchased from Invitrogen (Carlsbad, CA). The anti-HCV NS5A antibody was purchased from Bio-Design (Carmel, NY). The anti-HCV Core antibody was purchased from Affinity BioReagents (Golden, CO). The anti-β-actin antibody was purchased from Sigma (St. Louis, MO). The IFNα-2a was purchased from Roche (Mannheim, Germany). The 3-(4,5-dimethylthiazol-2-yl)-5-(3-carboxymethoxyphenyl)-2-(4-sulfophenyl)- 2H-tetrazolium (MTS) reduction assay and the luciferase assay reagents were purchased from Promega (Madison, WI).

Identification of liver miRNAs targeting the HCV genome

Bioinformatic strategy for the identification of liver miRNAs targeting the HCV genome is presented in Fig. 1. Briefly, two published miRNAs expression profiles [19, 20] were used to select for liver-abundant miRNAs. The miRNA is defined as liver abundance when the expression level of a specific liver miRNA divided by the average expression level of the total liver miRNAs is greater than one. The 23 miRNAs (Supplementary Table 1) that were identified as liver abundant in the two profiling databases were subject to bioinformatic analyses using miRanda, RNAhybrid, TargetScan, and PITA [21–24] to predict their target sequences on all six HCV genotypes (Supplementary Table 2). According to the calculation of miRanda, a filter was set to select for miRNAs of which the prediction scores for at least four genotypes were higher than 155. These miRNAs were considered as the candidate liver miRNAs targeting the HCV genome.

Cell culture and viability assay

Human hepatoma Huh7 cells were cultured in Dulbecco's modified Eagle's medium (DMEM) supplemented with 10% heat-inactivated fetal bovine serum (FBS). The Huh7.5 cells that represent a Huh7 subline and are highly permissive for HCV replication were maintained in DMEM with 1% non-essential amino acid (NEAA). The ConI cells were cultured in DMEM supplemented with 10% FBS and 750 μg/ml G418. The Huh7/Rep-Feo subgenome replicon cells were maintained in the same medium except that 1%

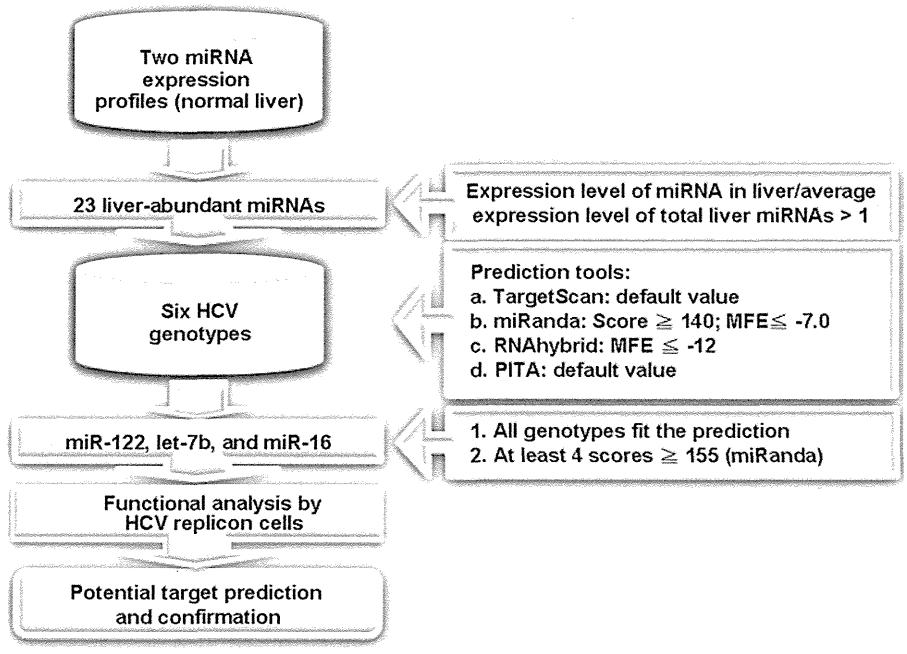

Fig. 1 Bioinformatic strategy for identifying liver miRNAs with target sites on HCV genome. Two published normal liver tissue miRNA expression profiles were used to select liver-abundant miRNAs for bioinformatics analyses as described in "Materials and methods"

NEAA was added and only 250 μg/ml G418 was used [25]. Viable cells were determined by the CellTiter 96 Aqueous One Solution Cell Proliferation Assay Kit.

Plasmid construction

For luciferase (luc) reporter plasmids, the predicted miRNA responsive element (MRE) for let-7b, as listed in Table 1, was inserted into the *Eco*RI/*Xba*I site downstream of the luciferase gene in phDab2-luc [26] to generate pluc-c-let-7b, pluc-MRE1, pluc-MRE2, pluc-MRE3, and pluc-MRE4. For generation of HCV subgenome mutants with nucleotide mismatch at the ''seed region'' of let-7b or "S1 binding site" of miR-122, site-directed mutagenesis was performed by QuickChange (Stratagene, CA) using pRep-Feo as the template [25] and the primer sets for mMRE1, mMRE2, mMRE3, and miR-122-mut as listed in Table 1. To generate a capped RNA transcript encoding firefly luciferase (FLuc) for use as an internal control in the transient translation assay, the FLuc gene from the plasmid pGL3-Promoter (Madison, WI) was first digested by the restriction enzyme *Nco*I. The nucleotides at the sticky end were filled up as blunt end by Klenow DNA polymerase and the FLuc gene was then excised by the restriction enzyme *Xba*I. On the other hand, pRL-TK plasmid was digested by *Nhe*I and the sticky end was filled up by Klenow DNA polymerase followed by *Xba*I restriction enzyme digestion to remove the Renilla luciferase gene (RLuc). The Fluc gene fragment was then cloned into pRL-TK to replace RLuc to generate pLUC-TK. This plasmid contains a T7 promoter and can transcribe mRNA after linearization by *Bam*HI.

Transient transfection and luciferase activity assay

For transient transfection, Huh7/Rep-Feo cells were seeded at a density of 1×10^4 cells/well for 24 h and the miRNA precursor or inhibitor was transfected into cells by LF2000. At 72 h after transfection, the luciferase activity was quantified using the Bright-Glo luciferase assay reagent. On the other hand, 293T cells were seeded at a density of 2×10^4 cells/well and the reporter plasmid, pRL-TK and miRNA precursor (100 nM) were cotransfected into cells by LF2000. At 24 h after transfection, the firefly and Renilla luciferase activities were quantified using the Dual-Glo luciferase assay reagent.

For RNA transfection, the *Xba*I-digested wild-type pRep-Feo or the mutant subgenome plasmid was subject to in vitro transcription for RNA synthesis. The Huh7.5 cells were transfected with 10 μg HCV RNA, 100 pmol miRNA, and 10 μg pRL-TK by electroporation using Gene Pulser II (Bio-Rad) at 260 V and 950 μF.

For permissive assay, Huh7 cells were seeded at a density of 2×10^5 cells/well and were transfected with the miRNA precursor (100 pmol) by RNAiMAX (Invitrogen) for 24 h. The transfected cells were subsequently infected with HCVcc (6×10^6 copies/ml) for 4 h. After washing away the virus, the cells were cultured for 72 h and the HCV RNA was detected from the infected cells by real-time reverse transcription-PCR (RT-PCR).

Table 1 The sequences for the primers used in this study

Primer name	Primer sequences	Size (mer)
For luciferase reporter constructs[a]		
c-let-7b	S:5′-CTAGA**AACCACACAACCTACTACCTCA**G-3′	22
	AS:5′-AATTC**TGAGGTAGTAGGTTGTGTGGTT**T-3′	
MRE1	S:5′-CTAGA**CACCATGAGCACGAATCCTAAACCTCA**G-3′	27
	AS: 5′-AATTC**TGAGGTTTAGGATTCGTGCTCATGGTG**T-3′	
MRE2	S: 5′-CTAGA**GGCAAAAGGGTGTACTACCTCA**G-3′	22
	AS: 5′-AATTC**TGAGGTAGTACACCCTTTTGCC**T-3′	
MRE3	S: 5′-CTAGA**AGCCACTTGACCTACCTCA**G-3′	19
	AS: 5′-AATTC**TGAGGTAGGTCAAGTGGCT**T-3′	
MRE4	S:5′-CTA**GAGCCGCATGACTGCAGAGAGTGCTGATACTGGCCTCT**G-3′	38
	AS: 5′-AATTC**AGAGGCCAGTATCAGCACTCTCTGCAGTCATGCGGCT**-3′	
For in vitro mutagenesis[b]		
mMRE1	F: 5′-GAGCACGAATCCTAA**TGGAGT**AAGAAAAACCAAAGG-3′	36
	R: 5′-CCTTTGGTTTTTCTT**ACTCCA**TTAGGATTCGTGCTC-3′	
mMRE2	F: 5′-CTGGCAAAAGGGTGTA**TTATC**TCACTCGCGATCCCAC-3′	47
	R: 5′-GTGGGATCGCGAGUGAG**ATAA**TACACCCTTTTGCCAG-3′	
mMRE3	F: 5′-CATTGAGCCACTTGACCT**TCCG**CAGATCATTGAACGACTC-3′	40
	R: 5′-GAGTCGTTCAATGATCTG**CGGA**AGGTCAAGTGGCTCAATG-3′	
miR-122 mut	F: 5′-CCCGATTGGGGGCGACAC**AG**CACCATAGATCACTCCCC-3′	38
	R: 5′-GGGGAGTGATCTATGGTG**CT**GTGTCGCCCCCAATCGGG-3′	
For synthesis of mature miRNA[c]		
7b	S: 5′UGAGGUAGUAGGUUGUGUGGUU 3′ AS:	22
	5′UUCCACACAACCUACUACCUCA 3′	
m7b	S: 5′UGA**A**CUA**A**UAGGUUGUGUGGUU 3′ AS:	22
	5′UUCCACACAACCUA**U**UA**G**UUCA 3′	

S sense strand, *AS* antisense strand *F* forward primer, *R* reverse primer

[a] The *bold letters* indicate the predicted sequence while the other sequence was generated for cloning into *EcoRI*/*XbaI* restriction enzyme site

[b,c] The *bold letters* indicate the mutated nucleotides

Ribonucleoprotein immunoprecipitation (RIP) assay

The RIP assay was performed using the miRNA isolation kit (Wako Laboratory Chemicals, Osaka, Japan) according to the manufacturer's instruction. Briefly, 10 μg of Rep-Feo subgenomic RNA was obtained by in vitro transcription and was co-transfected with 100 pmol of the indicated miRNA into Huh7.5 cells by electroporation. At 6 h after transfection, the cells were lysed in 1 ml of cell lysis solution (20 mM Tris–HCl, pH 7.4, 2.5 mM $MgCl_2$, 200 mM NaCl, and 0.05% NP40). After centrifugation, the supernatant was collected and mixed with anti-human Ago2 monoclonal antibody-conjugated agarose beads for 2 h at 4°C. After several washes with cell lysis solution, the HCV RNAs associated with Ago2-containing miRNA ribonucleoprotein (miRNP) complexes were eluted and were quantified by real-time RT-PCR. For knockdown of endogenous let-7b, the let-7b inhibitor (100 pmol) was transfected into Huh7.5 cells for 24 h followed by electroporation of the cells with the Rep-Feo HCV subgenomic RNA mutated at the miR-122 binding site (10 μg) and 100 pmol of let-7b inhibitor.

Western-blot analysis

The cell lysates were harvested and separated by 10% SDS-PAGE. The expression of HCV viral protein was detected using ECL kit (Perkin-Elmer) as described previously [27].

Production of HCVcc infectious particles and infectivity inhibition assay

The HCVcc infectious particle was produced as described previously [28]. Briefly, in vitro transcribed J6/JFH-based HCV genomic RNA was electroporated into Huh7.5 cells. The virus-containing supernatant was clarified by low-speed centrifugation, passed through a 0.45-μm filter, and concentrated by ultracentrifugation.

For infectivity inhibition assay, Huh7.5 cells were seeded in a six-swell plate at a density of 2×10^5 cells/well. At 24 h after plating, 100 nM miRNA was transfected into the cells using LF2000. HCVcc (0.1 MOI) was then added to each well for 4 h and the transfection complex was replaced with 2% FBS-containing medium for 72 h. The cells were fixed and stained by anti-Core antibody following by FITC-conjugated second antibody, counterstained with 4′,6-diamidino-2-phenylindole (DAPI), and the infectious foci were counted using fluorescence microscopy.

For JC1-Luc2A HCV reporter virus, Huh7.5 cells were seeded in a 96-well plate at a density of 1×10^4 cells/well. At 24 h after plating, HCV reporter virus (0.01 MOI) was added to each well for 4 h. Then 100 nM of the indicated miRNA was transfected into the infected cells using RNAiMax and the transfection complex was replaced with 2% FBS-containing medium for 72 h. The cell lysates were collected for luciferase activity and MTS assay.

RNA isolation and real-time quantitative RT-PCR

Total RNAs were extracted using ReZol method and were quantified using a NanoDrop spectrophotometer. For quantification of HCV RNA expression, total cellular RNA (100 ng) was subject to one-step RT-PCR (25 μl) containing 2× TaqMan master mix and the primer/probe set for HCV (HCV-F: 5′-TGCGGAACCGGTGAGTACA-3′, HCV-R: 5′-CTTAAGGTTTAGGATTCGTGCTCAT-3′, and probe: 5′-CACCCTATCAGGCAGTACCACAAGG CC-3′). The reaction condition was one cycle of 48°C for 30 min, one cycle of 95°C for 10 min, and 40 cycles of 95°C for 15 s followed by 60°C for 1 min using the ABI Prism 7000 Sequence Detection System. The expression of glyceraldehyde-3-phosphate dehydrogenase (GAPDH) was used as a normalization control. HCV RNA expression was quantified by the $\Delta\Delta C_t$ method, where C_t represented the threshold cycle.

The TaqMan® microRNA Assay System was used for miRNA detection and quantification. Briefly, the RT reaction was performed in a final volume of 15 μl containing 1.5 μl of 10× RT buffer, 2.5 μl of total RNA (25 ng), 3 μl of 5× miRNA-specific RT primer, 0.15 μl of 100 mM dNTP, 0.2 μl of 40 U/μl RNase inhibitor, and 1 μl of MultiScribe reverse transcriptase (50 U/μl). The reaction condition was 30 min at 16°C, 30 min at 42°C, and 5 min at 85°C. Real-time PCR was then performed in a 20-μl PCR containing 1.33 μl of RT product, 10 μl of 10× TaqMan Universal PCR master mix, and 1 μl of the primer and probe mix from the TaqMan® MicroRNA Assay Kit. The reaction condition was 95°C for 10 min followed by 40 cycles of 95°C for 15 s and 60°C for 60 s. The expression of RNU6B gene was used as the internal control.

HCV translation assay

Huh7.5 cells were seeded into a six-well plate at a density of 4×10^5 cells/well. At 24 h after transfection of let-7b miRNA (100 nM), the replication-deficient J6/JFH (p7-Rlu2A) GNN mutant RNA (1.25 μg/well) was transfected together with the capped and polyadenylated FLuc mRNA (125 ng/well) by LF2000. After 4 h, cells were harvested and dual luciferase activity assays were performed.

Statistical analysis

Statistical analysis was performed by Student's t test. $p < 0.05$ was considered as statistically significant.

Results

Identification and functional characterization of liver miRNAs with potential recognition sequences on HCV genome

A bioinformatic strategy as described in the "Materials and methods" section was developed to search for novel miRNAs with potential recognition sequences on HCV genome (Fig. 1). Three miRNAs including miR-122, let-7b, and miR-16 were uncovered. To elucidate whether these miRNAs have any functional effect on HCV infection, Huh7/Rep-Feo replicon cells (genotype 1b) were transfected with the indicated miRNAs and the luciferase activity was determined (Fig. 2a, b). In accord with a previous report [11], miR-122 enhanced HCV expression ($p < 0.05$). Notably, let-7b significantly suppressed HCV expression ($p < 0.01$) while miR-16 had only a moderate effect ($p = 0.343$).

To further confirm that let-7b can regulate HCV RNA accumulation, mutated let-7b (m7b) was designed to change three nucleotides on the wild-type let-7b sequences (Fig. 2b; Table 1). As calculated and predicted by miRanda, no m7b target sequence was found on HCV genome (data not shown). After transfection into Huh7/Rep-Feo replicon cells, m7b abrogated the inhibitory effect of let-7b on the luciferase activity (Fig. 2b) thereby demonstrating that let-7b is a negative regulator of HCV expression.

The effects of the three selected miRNAs on HCV expression were also evaluated using ConI replicon cells (Fig. 2c). These miRNAs were transfected into the replicon cells and the expression of viral proteins was determined at 72 h after transfection. Western-blot analysis revealed that miR-122 increased NS5A expression, while let-7b but not miR-16 caused a decrease in NS5A (Fig. 2c, left panel). Furthermore, the let-7b mutant form m7b lost its inhibitory effect on HCV and did not alter NS5A expression (Fig. 2c,

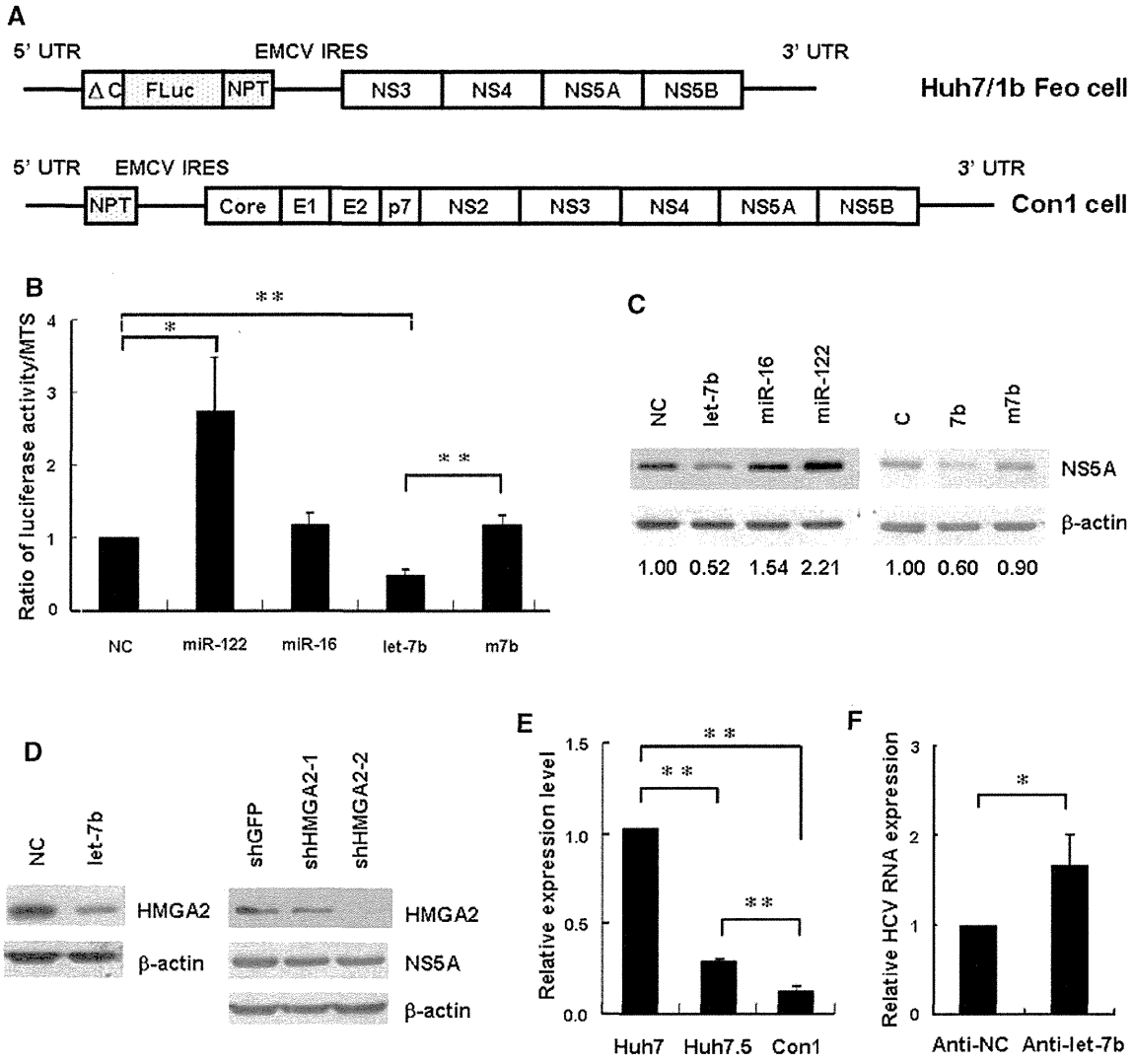

Fig. 2 Characterization of miRNAs with putative target sites on HCV genome. **a** Genomic structures of HCV maintaining in Huh7/Rep-Feo and ConI cells. **b** The miRNA precursors or mutant let-7b (m7b) were transfected into Huh7/Rep-Feo cells. MTS and luciferase activity assays were then performed at 72 h post-transfection. **c** The miRNA precursors (*left panel*) or the mutant form of let-7b (*right panel*) were transfected into the ConI cells. Western-blot analysis was then performed using the anti-NS5A and anti-β-actin antibody at 72 h post-transfection. The ratios for the relative band intensities of NS5A after normalization with β-actin were shown. *NC* negative control miRNA. **d** The precursors of let-7b (*left panel*) or shHMGA2 (*right panel*) were transfected into ConI replicon cells. Western-blot analysis was then performed using the anti-NS5A and anti-β-actin antibody at 72 h post-transfection. *NC* negative control miRNA. **e** Real-time RT-PCR of let-7b was performed using the total RNAs from the indicated cells. RNU6B was used as an internal control for normalization. The data represented the mean $\pm$ SD ($n = 3$; $^*p < 0.05$, $^{**}p < 0.01$, $^{***}p < 0.001$). **f** The let-7b inhibitor (Anti-let-7b) or control inhibitor (Anti-NC) was transfected into Huh7 cells, respectively. HCV RNA expression was quantified by real-time RT-PCR using the total RNAs from the indicated transfected cells. The expression of GAPDH was used as a control for normalization. The data represented the mean $\pm$ SD ($n = 3$; $^*p < 0.05$)

right panel). These data thereby implicate that let-7b elicits suppressive activity in HCV protein expression.

HMGA2 is one of the major let-7b target genes and is down-regulated in let-7b-transfected ConI cells as previous reported (Fig. 2d, left panel) [29]. To rule out down-regulation of host transcripts accounts for the inhibitory effect of let-7b on HCV expression, HMGA2 was knockdown by two independent shHMGA2 plasmids. Although HMGA2 was significantly down-regulated in the shHMGA2 expressing cells, no effect was observed for the expression of the viral protein NS5A (Fig. 2d, right panel). These data indicate that down-regulation of HMGA2 does not contribute to the effect of let-7b on HCV expression.

To further delineate the association between let-7b and HCV infectivity, let-7b expression in various HCV-associated cell lines were determined. As shown in Fig. 2e, let-7b expression in the HCV permissive Huh7.5 cells was less than its expression in the parental Huh7 cells ($p < 0.01$).

Consistent with these observations, ConI cells bearing replicated HCV genome also had much lower let-7b (Fig. 2e, $p < 0.01$). Furthermore, Huh7 cells were more permissive for HCVcc infection when let-7b was inactivated by the let-7b inhibitor (Fig. 2f, $p < 0.05$). These data indicate that the cells capable of persistent HCV replication are usually associated with a low level of let-7b expression.

Let-7b reduces HCVcc infectivity

The HCVcc system was used to elucidate the role of let-7b in HCV infectivity. Let-7b was transfected into Huh7.5 cells followed by infection with HCVcc derived from J6/JFH-1 (genotype 2a). Hepatitis C virus expression was then monitored by fluorescent staining using the anti-HCV Core antibody (Fig. 3a). Our data revealed that let-7b reduced HCV infectivity for 42% ($p < 0.05$) while miR-122 enhanced the infectivity for 63% ($p < 0.05$) when compared to the cells expressing negative control miRNA (Fig. 3b). The HCV RNA was also decreased in let-7b-transfected cells (Fig. 3c, $p < 0.05$) indicating that let-7b suppresses HCV RNA level leading to a decrease in viral production.

To further confirm the negative regulatory effect of let-7b on HCVcc production, Huh7.5 cells were infected with the JC1-Luc2A HCV reporter virus and the luciferase activity was used to evaluate HCV viral production. Our data revealed that let-7b reduced 75% of the HCV reporter virus luciferase activity (Fig. 3d, $p < 0.001$) when compared to the cells expressing negative control miRNA. As a control, miR-122 increased 87% of the HCV reporter virus luciferase activity ($p < 0.05$). In contrast, mutation of

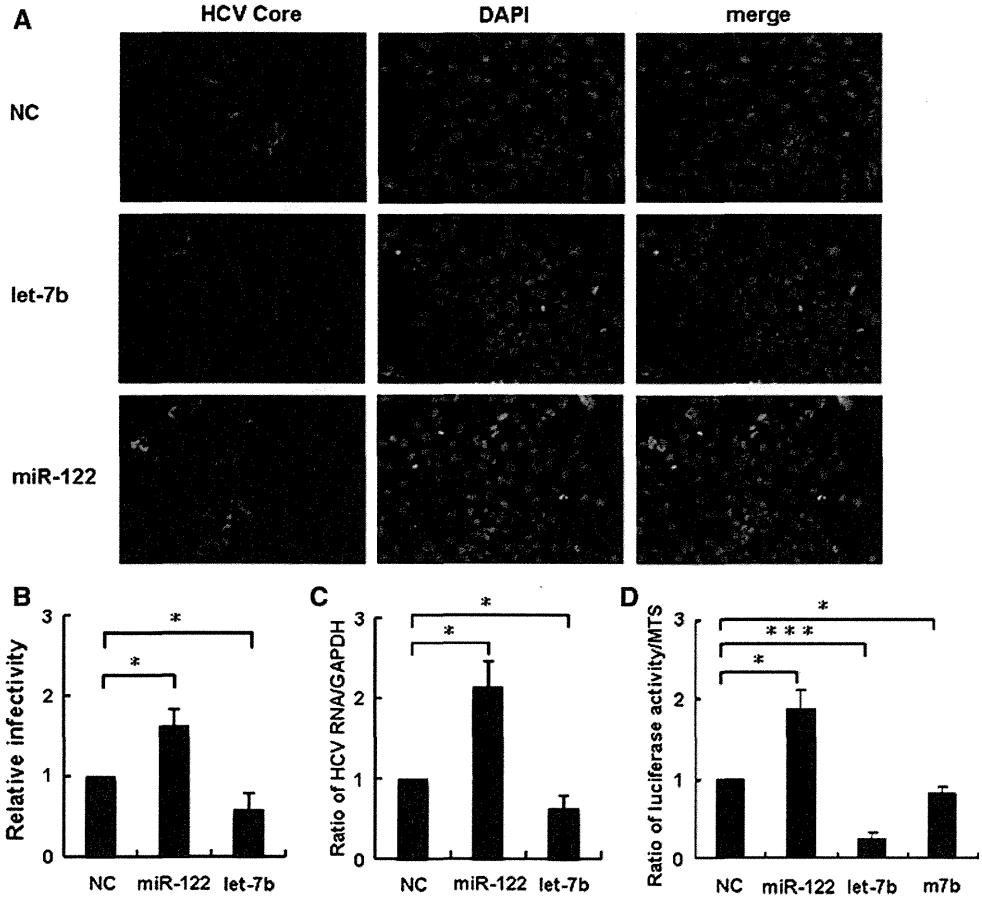

Fig. 3 Let-7b reduces HCVcc infectivity. **a** The indicated miRNAs were transfected into Huh7.5 cells for 24 h followed by infection with J6/JFH-based HCVcc. After 72 h, the cells were stained by anti-Core antibody. Nuclei were visualized by DAPI staining. *NC* negative control. **b** The infectious foci were counted by fluorescence microscopy. The infectivity for the cells transfected with negative control miRNA (NC) was set as one. The data represented the mean ± SD ($n = 3$; $^*p < 0.05$). **c** HCV RNA expression was quantified by real-time RT-PCR using the total RNAs from the indicated transfected cells. The expression of GAPDH was used as a control for normalization. The data represented the mean ± SD ($n = 3$; $^*p < 0.05$). **d** The miRNA precursors or the mutant let-7b (m7b) were transfected into Huh7.5 cells for 24 h followed by infection with JC1-luc2A HCV reporter virus. After 72 h, cell viability was determined by MTS assay and the cell extracts were collected for luciferase activity assay. The relative firefly luciferase versus MTS activity was shown and the negative control miRNA was arbitrarily denoted as one. The data represented the mean ± SD ($n = 3$; $^*p < 0.05$; $^{***}p < 0.001$)

let-7b (m7b) diminished its inhibitory effect on HCV expression and resulted in a slight inhibition of HCV reporter virus luciferase activity ($p < 0.05$). Together, these data implicate that inhibition of HCV RNA expression accounts for the suppressive effect of let-7b on HCV infection.

Let-7b physically interacts with the HCV genome

Argonaute 2 is the core component of miRNA-induced silencing complex (miRISC), which binds the guide miRNA to silence target mRNAs [30]. To determine whether Ago2 together with let-7b and HCV RNA form a miRISC complex, HCV RNA was co-transfected with let-7b into Huh7.5 cells followed by immunoprecipitation using the anti-Ago2 antibody (Ago2-IP). Because the "site 1" sequence (Table 1) is the most important HCV genome sequence for miR-122 binding and for regulation of HCV by miR-122, "site 1" mutation S1-p34 m (miR-122-mut) [11, 12] was introduced into the HCV subgenome to minimize the interference from the endogenous miR-122. The amount of Ago2-IP-associated HCV RNA was quantified by real-time RT-PCR. As shown in Fig. 4a, both HCV RNA subgenomes with wild-type or mutant miR-122 binding site were found to associate with the miRNP complex, while let-7b promoted HCV-miRNP interactions when miR-122 binding site was mutated. The total amount of let-7b associating with the Ago2-IP fraction was unchanged (Fig. 4b). Furthermore, knockdown of endogenous let-7b in Huh7.5 cells followed by Ago2-IP revealed that both the amounts of HCV RNA (Fig. 4c) and let-7b (Fig. 4d) in the Ago2-IP fraction were dramatically decreased. These data thereby indicate that let-7b physically interacts with HCV RNA in the Ago2-containing miRNP complex.

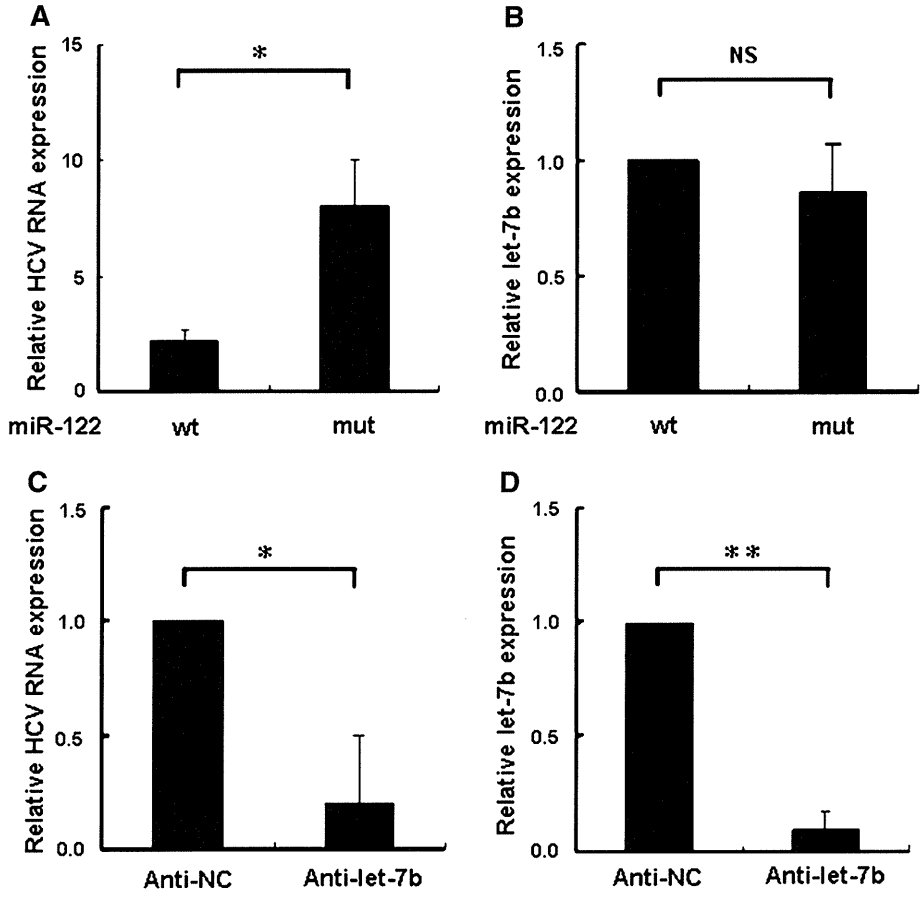

Fig. 4 Let-7b is associated with HCV genome in miRNP complex. **a**, **b** Huh7.5 cells were transfected with 100 pmol of miRNA along with 10 μg of either wild-type (miR-122-wt) or mutant (miR-122-mut) HCV subgenome RNA. The cell extracts were collected to perform co-immunoprecipitation with the anti-Ago2 antibody (Ago2-IP). HCV replicon RNA (*panel* **a**) and let-7b (*panel* **b**) were measured by real-time RT-PCR using total RNA sample from the Ago2-IP fraction. **c** ,**d** For knockdown of endogenous let-7b, Huh7.5 cells were transfected with 100 pmol of the indicated miRNA inhibitors (Anti-NC and Anti-let-7b) for 24 h followed by electroporation of the cells with 10 μg of miR-122-mut and 100 pmol of the indicated miRNA inhibitors. The cell extracts were collected to perform Ago2-IP and the HCV replicon RNA (*panel* **c**) and let-7b (*panel* **d**) were measured by real-time RT-PCR. The relative levels for HCV RNA and let-7b in the Ago2-IP complexes were shown. The data represented the mean ± SD ($n = 3$; $*p < 0.05$, $**p < 0.01$)

Identification of let-7b-responsive elements on the HCV genome

To identify MRE for let-7b, HCV-N genomic sequences (genotype 1b) were subject to bioinformatic prediction using miRanda and RNAhybrid. Several putative MREs for let-7b were revealed (Fig. 5a; Supplementary Tables 3, 4). It is noted that MRE2 (nt 8,745–8,766) and MRE3 (nt 8,977–8,995) that located within the HCV NS5B coding region had the highest prediction score and were selected for analysis. Moreover, the MRE1 (nt 338–365) and MRE4 (nt 9,566–9,603) at the non-coding region that had the lowest minimum free energies (MFE) in NCR region (Table 2) were also subject to further analysis.

To determine whether any of these sequences is the authentic MREs for let-7b, luciferase reporter plasmids with the reported let-7b target sequence (pluc-let-7b) and the putative MREs in HCV genome were constructed (pluc-MRE1, pluc-MRE2, pluc-MRE3, and pluc-MRE4). After co-transfection with let-7b or a negative control miRNA into 293T cells, the luciferase activities for each individual reporter plasmid were measured. Our data revealed that let-7b decreased pluc-MRE1, pluc-MRE2, and pluc-MRE3 luciferase activity by 28, 31, and 37%, respectively (Fig. 5b). No effect was found for pluc-MRE4. These data indicate that the MRE1, MRE2, and MRE3 are the potential let-7b binding sites on HCV genome.

Mutations of the putative let-7b MREs were introduced into the HCV subgenome to exam whether these MREs are responsible for the suppressive effect of let-7b. Silent mutations of MRE2 and MRE3 were designed to avoid amino acid changes while a six-nucleotide substitution mutation was introduced into HCV Rep-Feo subgenome (wild-type) to generate mMRE1, mMRE2, mMRE3, and mMRE2,3, respectively. Structural analysis of these mutations revealed that most of the HCV RNA genome structures were maintained except that mMRE1 appeared

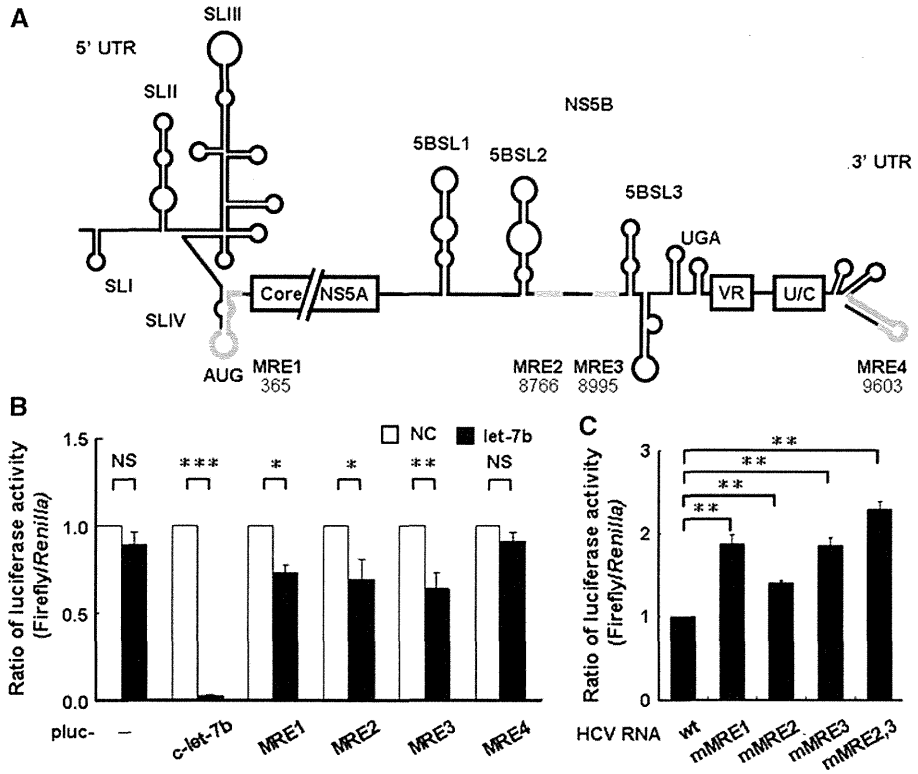

Fig. 5 The MREs of let-7b are located at the NS5B coding sequences and 5′-UTR of HCV genome. **a** Schematic representation for the predicted MREs of let-7b on HCV genome. The *number* corresponds to the first nucleotide of the predictive seed region. **b** The precursor of let-7b or negative control miRNA (NC) was co-transfected with the indicated luciferase reporter plasmid and pRL-TK into 293T cells for 24 h. The luciferase activities were measured and the relative firefly versus Renilla luciferase activity was shown. The plasmid containing perfect complementary sequence of let-7b (c-let-7b) and the vector control reporter plasmid (luciferase activity arbitrarily denoted as one) was used as the positive and negative control, respectively. The data represented the mean ± SD ($n = 3$; $*p < 0.05$; $**p < 0.01$; $***p < 0.001$; *NS* no significance). **c** The RNAs for wild-type (wt) HCV genome and the genome with mutations at the indicated MREs regions were obtained by in vitro transcription and were transfected individually into Huh7.5 cells along with let-7b precursor or negative control miRNA (NC) by electroporation. The luciferase activity was determined at 96 h post-transfection. The luciferase activity generated by wild-type HCV genome was arbitrarily denoted as 1 and the luciferase activity derived from each mutant HCV genome normalized by luciferase activity from wild-type was shown. The data represented the mean ± SD ($n = 3$; $**p < 0.01$)

Table 2 Characterization of let-7b predicted binding sites on HCV genome

MRE	Secondary structure	MFE[a]	Score[a]	Position (HCV-N)
MRE1	miRNA 3'-UUGG----UGUGUU--GGAUGAUGGAGU-5' Target 5'-CACCAUGAGCACGAAUCCUAA-ACCUCAA-3'	-26	84	338-365
MRE2	miRNA 3'-UUGGUGUGUUGGAUGAUGGAGU-5' Target 5'-GGCAAAAGGGUGUACUACCUCA-3'	-16.7	156	8745-8766
MRE3	miRNA 3'-UUGGUGUGUUGGAUGAUGGAGU-5' Target 5'-AGCCACUUGAC---CUACCUCA-3'	-21.1	152	8977-8995
MRE4	miRNA 3'-UUGGUGUGUUGG----------AUGA-UGGAGU-5' Target 5'GAGCCGCAUGACUGCAGAGAGUGCUGAUACUGGCCUCU-3'	-28.5	93	9566-9603

[a] MFE was calculated by RNAhybrid while Score was calculated by miRanda

to generate a small stem-loop structure (Supplementary Fig. S1). These mutated HCV RNAs were obtained by in vitro transcription and, together with let-7b, electroporated into Huh7.5 followed by analysis of luciferase activity. Our data revealed that the luciferase activities for HCV subgenome with mMRE1, mMRE2, and mMRE3 were 87, 40, and 86% higher than the wild-type HCV subgenome, respectively (Fig. 5c), implicating that let-7b-mediated suppression of HCV replicon activity is abrogated by mutating the target sequences on HCV genome. Moreover, HCV subgenome with double mutations of MRE2 and MRE3 synergistically enhanced luciferase activity when compared to the single mutant for these two MREs. The RNA structure did not contribute to the loss of let-7b responsiveness because Mfold analysis demonstrated that the wild-type and mutant HCV subgenome had similar RNA structure (Supplement Fig. S1). These data thereby indicate that 5′-UTR and NS5B coding sequences contain let-7b binding sites.

The antiviral effect of let-7b is independent of inhibition of HCV translation

It has been reported that miR-122 enhances HCV replication by stimulating internal ribosome entry site (IRES)-mediated translation in cultured cells [12]. Because MRE1 is located at domain IV of IRES [31], the possibility of let-7b modulating HCV replication through translation was also examined. The replication-deficient J6/JFH (p7-Rlu2A) GNN HCV mutant RNA was transfected along with a capped and polyadenylated FLuc mRNA as an internal control for transfection and translation. The ratio of Renilla luciferase (RLuc) to firefly luciferase (FLuc) activity was used to measure the IRES-directed translation activity. As shown in Fig. 6, miR-122 enhanced HCV IRES activity for approximate threefold, while miR-122 inhibitor resulted in approximate 50% decrease of the activity. However, let-7b or its inhibitor had no effects on HCV translation (Fig. 6). These data indicate that let-7b regulates HCV RNA replication through a mechanism independent of HCV translational regulation.

Let-7b and INFα-2a elicit synergistic anti-HCV activity

We examined further whether there is a synergistic effect between let-7b and IFNα-2a. The Huh7/Rep-Feo cells were treated with different concentrations of IFNα-2a and the luciferase activity for HCV subgenome was measured to determine the optimized dosage of IFNα-2a for synergistic study. As shown in Fig. 7a, the luciferase activity was suppressed by IFNα-2a in a dose-dependent manner with the IC50 equivalent to 1.39 ng/ml. When Huh7/Rep-Feo cells were transfected with let-7b followed by treatment with IFNα-2a, a 60 and 70% decrease in luciferase activity was observed in relative to let-7b or IFNα-2a alone, respectively (Fig. 7b, $p < 0.01$). These data thereby indicate that let-7b and IFNα-2a elicit synergistic inhibitory effect on HCV expression.

Discussion

The interplays between viral infection and miRNA have been demonstrated since the first report unfolding miR-32 as the negative regulator of primate foamy virus RNA accumulation [32]. Subsequently a number of miRNAs

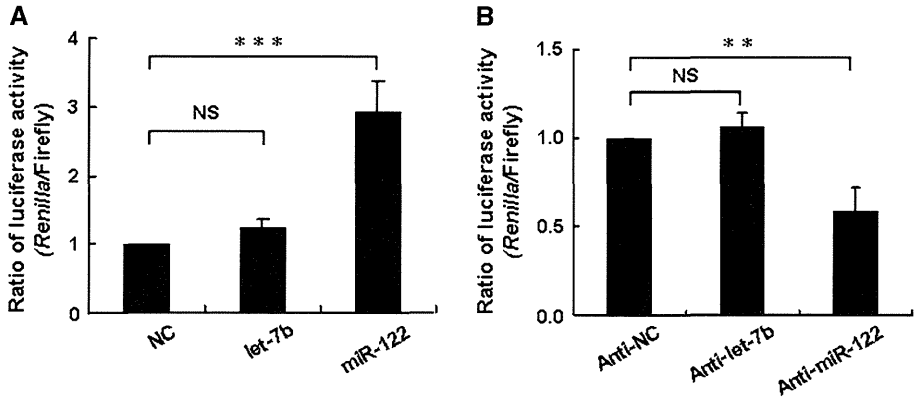

Fig. 6 Let-7b decreases HCV RNA expression independent on translation inhibition. **a, b** Huh7.5 cells were transfected with the indicated miRNAs (*panel* **a**) or miRNA inhibitors (*panel* **b**). Twenty-four hour later, HCV RNAs carrying GND mutation and Renilla luciferase coding sequence were transfected with a capped and polyadenylated firefly luciferase mRNA. At 4 h after transfection, the cell lysates were subject to dual luciferase activity assays. The relative firefly versus Renilla luciferase activity is shown. The data represented the mean ± SD ($n = 3$; $^{**}p < 0.01$; $^{***}p < 0.001$; *NS* no significance)

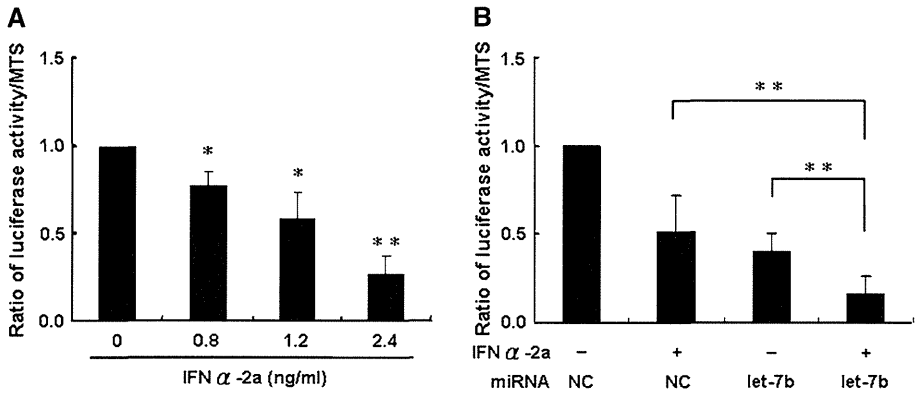

Fig. 7 Let-7b and IFNα-2a elicit synergistic inhibitory effects on HCV RNA accumulation. **a** Huh7/Rep-Feo cells (3×10^4) were treated with the indicated doses of IFN-2α for 72 h and the luciferase activity and cell viability were determined. **b** Huh7/Rep-Feo cells were transfected with 100 nM of let-7b or negative control miRNA (NC) by RNAiMAX for 4 h followed by treatment with INF-2α or medium control for additional 72 h. The luciferase activity and cell viability were determined. The data represented the mean ± SD ($n = 3$) with the luciferase activity normalized by the cell viability. ($^{*}p < 0.05$; $^{**}p < 0.01$)

were found to elicit anti-HCV activity [11, 13, 14]. In this study, bioinformatic tools and virological analyses are employed to unveil novel cellular miRNAs associated with HCV infection. We demonstrate that, in addition to miR-122 that has been reported to augment HCV infection, let-7b targets the HCV genome leading to a decrease in HCV RNA accumulation and viral production. This study thereby represents the first report to identify let-7b as a negative regulator of HCV infection.

Let-7b is the first known human miRNA [33] that is closely associated with the status of cellular differentiation and is usually down-regulated in cancers [34, 35]. Experimental evidence we present in this study unveils the role of let-7b in the control of HCV pathogenesis. Let-7b expression is irreversibly correlated with HCV infectivity in the cell-based systems; the cell lines bearing replicated HCV genome that are permissive for HCV replication (such as Huh7.5 and Con1) usually have low levels of let-7b expression. Moreover, let-7b is associated with HCV genome in Ago2 miRNP complex. Cellular study further reveals that let-7b diminishes luciferase reporter gene expression in Huh7/Rep-Feo subgenome replicon (1b genotype), the viral protein expression in ConI replicon (1b genotype) and HCV RNA accumulation and viral production upon HCVcc infection (2a genotype). These findings not only indicate that let-7b plays a role in the host antiviral response, but also reveal the universal effects of let-7b on different HCV genotypes.

The molecular basis for the anti-HCV effect of let-7b is also elucidated in this study. Our data support the notion that let-7b directly interacts with the HCV genome and modulates virus production. Although a number of miRNAs have been reported to regulate HCV replication and pathogenesis, only miR-122 and miR199a* were

demonstrated to directly target on HCV genome [11, 13]. Let-7b thereby represents the third cellular miRNA that elicits a direct effect on HCV genome and modulates HCV replication. In contrast to miR-122 and miR-199a*, of which the target sequences mapped to 5′-UTR [11, 13], one of the unique features for let-7b is that two of the let-7b target sequences, MRE2 and MRE3, are located within the coding region of NS5B. Although it is not common, miRNA has been shown to affect gene expression by interacting with mRNA coding regions [36, 37]. For example, miR-148 and miR-24 repress DNA methyltransferase 3b and p16 expression, respectively, primarily through the coding region recognition site [38, 39]. Let-7b targets the coding sequence of Dicer and establishes a miRNA/Dicer autoregulatory negative feedback loop. While the advantages for let-7b targeting the HCV coding sequence remain to be elucidated, let-7b symbolizes the first cellular miRNA with recognition sequences in the coding region of the HCV genome.

Although our data indicate that let-7b acts on the HCV genome leading to a decrease in HCV expression, we cannot rule out that the host factors regulated by let-7b may also play a role in the regulation of HCV expression. Several host factors are down-regulated by let-7b, including HMGA2 [40–42]. Moreover, TargetScan prediction reveals at least 79 cellular target genes regulated by let-7b have some associations with HCV infection. Despite that knockdown of HMGA2 does not have any effect of HCV protein expression, whether the other host factors mediating let-7b effects on HCV expression remains to be investigated.

While only let-7b meets our preset selection criteria, bioinformatic prediction data reveal that three other family members of let-7, including let-7a, let-7c, and let-7f, are also liver-abundant (Supplementary Table 1). Because let-7 family members differ by only one to a few nucleotides [43], let-7a, let-7c, and let-7f were also tested for their potential effects on HCV expression. As shown in Supplementary Fig. S2, let-7a and let-7f were expressed at a lower level in HCV-sensitive cell lines while let-7c was expressed at a higher level. In addition, these three miRNAs can also reduce HCV activity on subgenome replicon cells and reporter virus. However, let-7b exhibits more prominent suppressive effects than the others. Hence, it is likely that let-7 family members may act on HCV in a similar way to let-7b with various regulations.

In addition to controlling multiple cellular events, miRNA has been proposed as a therapeutic regimen for various diseases [44, 45]. Recently, a locked nucleic acid-modified oligonucleotide complementary to miR-122 exhibits a long-lasting suppression of HCV viremia in chronically infected chimpanzees [46]. Small-molecule inhibitors and activators of miR-122 have been developed to reduce HCV viral replication [47]. In this study, we found that let-7b plays a role in host defense to combat HCV infection and reduces HCV infectivity. The synergistically inhibitory effect of let-7b and IFNα-2a on HCV replication further implies that let-7b is a good candidate for developing an adjuvant regimen for IFNα-2a in a clinical setting.

In conclusion, we demonstrate for the first time that let-7b inhibits HCV expression and replication by targeting the conserved HCV 5′UTR and coding region. Furthermore, let-7b and IFNα-2a elicit synergistically inhibitory effect on HCV infection. This study thereby contributes to our understanding for let-7b on the control of HCV pathogenesis and offers new insight for developing novel anti-HCV therapeutic approaches.

Acknowledgments The authors thank Dr. Naoya Sakamoto for providing HCV subgenome replicon cells, Professor Charles Rice (The Rockefeller University, USA) for providing ConI replicon, Huh7.5 cells, and plasmids pFL-J6/JFH, pJ6/JFH(p7-Rluc2A), Professor Robert T. Schooley (University of California-San Diego) for providing plasmid pJC1-Luc2A (with the permission of Apath). This work was supported in part by grants NSC 97-2320-B-039-026-MY3 and NSC 100-2320-B-039-007-MY3 (J.C.C.) and part by NSC-100-2911-I-009-101 (H.D.H.) from the National Science Council and part by Chang Gung Molecular Medicine Research Center Grant (C.P.T.).

Conflict of interest None.

References

1. Poynard T, Yuen MF, Ratziu V, Lai CL (2003) Viral hepatitis C. Lancet 362:2095–2100
2. Lavanchy D (2009) The global burden of hepatitis C. Liver Int 29(Suppl 1):74–81
3. Manns MP, Wedemeyer H, Cornberg M (2006) Treating viral hepatitis C: efficacy, side effects, and complications. Gut 55:1350–1359
4. Sarrazin C, Kieffer TL, Bartels D, Hanzelka B, Muh U, Welker M, Wincheringer D, Zhou Y, Chu HM, Lin C, Weegink C, Reesink H, Zeuzem S, Kwong AD (2007) Dynamic hepatitis C virus genotypic and phenotypic changes in patients treated with the protease inhibitor telaprevir. Gastroenterology 132:1767–1777
5. De Francesco R, Migliaccio G (2005) Challenges and successes in developing new therapies for hepatitis C. Nature 436:953–960
6. Ng TI, Mo H, Pilot-Matias T, He Y, Koev G, Krishnan P, Mondal R, Pithawalla R, He W, Dekhtyar T, Packer J, Schurdak M, Molla A (2007) Identification of host genes involved in hepatitis C virus replication by small interfering RNA technology. Hepatology 45:1413–1421
7. Ambros V (2004) The functions of animal microRNAs. Nature 431:350–355
8. Bartel DP (2009) MicroRNAs: target recognition and regulatory functions. Cell 136:215–233
9. Gottwein E, Cullen BR (2008) Viral and cellular microRNAs as determinants of viral pathogenesis and immunity. Cell Host Microbe 3:375–387

10. Randall G, Panis M, Cooper JD, Tellinghuisen TL, Sukhodolets KE, Pfeffer S, Landthaler M, Landgraf P, Kan S, Lindenbach BD, Chien M, Weir DB, Russo JJ, Ju J, Brownstein MJ, Sheridan R, Sander C, Zavolan M, Tuschl T, Rice CM (2007) Cellular cofactors affecting hepatitis C virus infection and replication. Proc Natl Acad Sci USA 104:12884–12889
11. Jopling CL, Yi M, Lancaster AM, Lemon SM, Sarnow P (2005) Modulation of hepatitis C virus RNA abundance by a liver-specific MicroRNA. Science 309:1577–1581
12. Jangra RK, Yi M, Lemon SM (2010) Regulation of hepatitis C virus translation and infectious virus production by the microRNA miR-122. J Virol 84:6615–6625
13. Murakami Y, Aly HH, Tajima A, Inoue I, Shimotohno K (2009) Regulation of the hepatitis C virus genome replication by miR-199a. J Hepatol 50:453–460
14. Pedersen IM, Cheng G, Wieland S, Volinia S, Croce CM, Chisari FV, David M (2007) Interferon modulation of cellular microRNAs as an antiviral mechanism. Nature 449:919–922
15. Wilson JA, Zhang C, Huys A, Richardson CD (2011) Human Ago2 is required for efficient microRNA 122 regulation of hepatitis C virus RNA accumulation and translation. J Virol 85:2342–2350
16. Jangra RK, Yi M, Lemon SM (2010) DDX6 (Rck/p54) is required for efficient hepatitis C virus replication but not for internal ribosome entry site-directed translation. J Virol 84:6810–6824
17. Jones CT, Murray CL, Eastman DK, Tassello J, Rice CM (2007) Hepatitis C virus p7 and NS2 proteins are essential for production of infectious virus. J Virol 81:8374–8383
18. Blight KJ, McKeating JA, Rice CM (2002) Highly permissive cell lines for subgenomic and genomic hepatitis C virus RNA replication. J Virol 76:13001–13014
19. Hsu SD, Chu CH, Tsou AP, Chen SJ, Chen HC, Hsu PW, Wong YH, Chen YH, Chen GH, Huang HD (2008) miRNAMap 2.0: genomic maps of microRNAs in metazoan genomes. Nucleic Acids Res 36:D165–D169
20. Liang Y, Ridzon D, Wong L, Chen C (2007) Characterization of microRNA expression profiles in normal human tissues. BMC Genomics 8:166–187
21. John B, Enright AJ, Aravin A, Tuschl T, Sander C, Marks DS (2004) Human MicroRNA targets. PLoS Biol 2:e363
22. Rehmsmeier M, Steffen P, Hochsmann M, Giegerich R (2004) Fast and effective prediction of microRNA/target duplexes. RNA 10:1507–1517
23. Lewis BP, Shih IH, Jones-Rhoades MW, Bartel DP, Burge CB (2003) Prediction of mammalian microRNA targets. Cell 115:787–798
24. Kertesz M, Iovino N, Unnerstall U, Gaul U, Segal E (2007) The role of site accessibility in microRNA target recognition. Nat Genet 39:1278–1284
25. Tanabe Y, Sakamoto N, Enomoto N, Kurosaki M, Ueda E, Maekawa S, Yamashiro T, Nakagawa M, Chen CH, Kanazawa N, Kakinuma S, Watanabe M (2004) Synergistic inhibition of intracellular hepatitis C virus replication by combination of ribavirin and interferon-alpha. J Infect Dis 189:1129–1139
26. Tseng CP, Huang CH, Tseng CC, Lin MH, Hsieh JT, Tseng CH (2001) Induction of disabled-2 gene during megakaryocyte differentiation of K562 cells. Biochem Biophys Res Commun 285:129–135
27. Cheng JC, Chang MF, Chang SC (1999) Specific interaction between the hepatitis C virus NS5B RNA polymerase and the 3′ end of the viral RNA. J Virol 73:7044–7049
28. Wakita T, Pietschmann T, Kato T, Date T, Miyamoto M, Zhao Z, Murthy K, Habermann A, Krausslich HG, Mizokami M, Bartenschlager R, Liang TJ (2005) Production of infectious hepatitis C virus in tissue culture from a cloned viral genome. Nat Med 11:791–796
29. Lee YS, Dutta A (2007) The tumor suppressor microRNA let-7 represses the HMGA2 oncogene. Genes Dev 21:1025–1030
30. Chendrimada TP, Gregory RI, Kumaraswamy E, Norman J, Cooch N, Nishikura K, Shiekhattar R (2005) TRBP recruits the Dicer complex to Ago2 for microRNA processing and gene silencing. Nature 436:740–744
31. Berry KE, Waghray S, Doudna JA (2010) The HCV IRES pseudoknot positions the initiation codon on the 40S ribosomal subunit. RNA 16:1559–1569
32. Lecellier CH, Dunoyer P, Arar K, Lehmann-Che J, Eyquem S, Himber C, Saib A, Voinnet O (2005) A cellular microRNA mediates antiviral defense in human cells. Science 308:557–560
33. Pasquinelli AE, Reinhart BJ, Slack F, Martindale MQ, Kuroda MI, Maller B, Hayward DC, Ball EE, Degnan B, Muller P, Spring J, Srinivasan A, Fishman M, Finnerty J, Corbo J, Levine M, Leahy P, Davidson E, Ruvkun G (2000) Conservation of the sequence and temporal expression of let-7 heterochronic regulatory RNA. Nature 408:86–89
34. Takamizawa J, Konishi H, Yanagisawa K, Tomida S, Osada H, Endoh H, Harano T, Yatabe Y, Nagino M, Nimura Y, Mitsudomi T, Takahashi T (2004) Reduced expression of the let-7 microRNAs in human lung cancers in association with shortened postoperative survival. Cancer Res 64:3753–3756
35. Yu F, Yao H, Zhu P, Zhang X, Pan Q, Gong C, Huang Y, Hu X, Su F, Lieberman J, Song E (2007) let-7 regulates self renewal and tumorigenicity of breast cancer cells. Cell 131:1109–1123
36. Forman JJ, Coller HA (2010) The code within the code: MicroRNAs target coding regions. Cell Cycle 9:1533–1541
37. Huang S, Wu S, Ding J, Lin J, Wei L, Gu J, He X (2010) MicroRNA-181a modulates gene expression of zinc finger family members by directly targeting their coding regions. Nucleic Acids Res 38:7211–7218
38. Duursma AM, Kedde M, Schrier M, le Sage C, Agami R (2008) miR-148 targets human DNMT3b protein coding region. RNA 14:872–877
39. Lal A, Kim HH, Abdelmohsen K, Kuwano Y, Pullmann R Jr, Srikantan S, Subrahmanyam R, Martindale JL, Yang X, Ahmed F, Navarro F, Dykxhoorn D, Lieberman J, Gorospe M (2008) p16(INK4a) translation suppressed by miR-24. PLoS One 3:e1864
40. Forman JJ, Legesse-Miller A, Coller HA (2008) A search for conserved sequences in coding regions reveals that the let-7 microRNA targets Dicer within its coding sequence. Proc Natl Acad Sci USA 105:14879–14884
41. Mahajan A, Liu Z, Gellert L, Zou X, Yang G, Lee P, Yang X, Wei JJ (2010) HMGA2: a biomarker significantly overexpressed in high-grade ovarian serous carcinoma. Mod Pathol 23:673–681
42. Zhao C, Sun G, Li S, Lang MF, Yang S, Li W, Shi Y (2010) MicroRNA let-7b regulates neural stem cell proliferation and differentiation by targeting nuclear receptor TLX signaling. Proc Natl Acad Sci USA 107:1876–1881
43. Roush S, Slack FJ (2008) The let-7 family of microRNAs. Trends Cell Biol 18:505–516
44. Branch AD, Rice CM (2010) Antisense gets a grip on miR-122 in chimpanzees. Sci Transl Med 2:13ps11
45. Jackson A, Linsley PS (2010) The therapeutic potential of microRNA modulation. Discov Med 9:311–318
46. Lanford RE, Hildebrandt-Eriksen ES, Petri A, Persson R, Lindow M, Munk ME, Kauppinen S, Orum H (2010) Therapeutic silencing of microRNA-122 in primates with chronic hepatitis C virus infection. Science 327:198–201
47. Young DD, Connelly CM, Grohmann C, Deiters A (2010) Small molecule modifiers of microRNA miR-122 function for the treatment of hepatitis C virus infection and hepatocellular carcinoma. J Am Chem Soc 132:7976–7981

JVI
Journals.ASM.org

Novel Cell Culture-Adapted Genotype 2a Hepatitis C Virus Infectious Clone

Tomoko Date,[a] Takanobu Kato,[a] Junko Kato,[b] Hitoshi Takahashi,[a]* Kenichi Morikawa,[a,c]* Daisuke Akazawa,[a,d] Asako Murayama,[a] Keiko Tanaka-Kaneko,[e] Tetsutaro Sata,[e]* Yasuhito Tanaka,[f] Masashi Mizokami,[g] and Takaji Wakita[a]

Department of Virology II, National Institute of Infectious Diseases, Tokyo,[a] Institute of Geriatrics, Tokyo Women's Medical University, Tokyo,[b] Division of Gastroenterology, Department of Medicine, Showa University School of Medicine, Tokyo,[c] Pharmaceutical Research Laboratories, Toray Industries, Inc., Kanagawa,[d] Department of Pathology, National Institute of Infectious Diseases, Tokyo,[e] Department of Virology and Liver Unit, Nagoya City University Graduate School of Medical Sciences, Nagoya,[f] and The Research Center for Hepatitis and Immunology, National Center for Global Health and Medicine, Chiba,[g] Japan

Although the recently developed infectious hepatitis C virus system that uses the JFH-1 clone enables the study of whole HCV viral life cycles, limited particular HCV strains have been available with the system. In this study, we isolated another genotype 2a HCV cDNA, the JFH-2 strain, from a patient with fulminant hepatitis. JFH-2 subgenomic replicons were constructed. HuH-7 cells transfected with *in vitro* transcribed replicon RNAs were cultured with G418, and selected colonies were isolated and expanded. From sequencing analysis of the replicon genome, several mutations were found. Some of the mutations enhanced JFH-2 replication; the 2217AS mutation in the NS5A interferon sensitivity-determining region exhibited the strongest adaptive effect. Interestingly, a full-length chimeric or wild-type JFH-2 genome with the adaptive mutation could replicate in Huh-7.5.1 cells and produce infectious virus after extensive passages of the virus genome-replicating cells. Virus infection efficiency was sufficient for autonomous virus propagation in cultured cells. Additional mutations were identified in the infectious virus genome. Interestingly, full-length viral RNA synthesized from the cDNA clone with these adaptive mutations was infectious for cultured cells. This approach may be applicable for the establishment of new infectious HCV clones.

Hepatitis C virus (HCV) is a principal agent in posttransfusion and sporadic acute hepatitis (6, 19). HCV belongs to the *Flaviviridae* family and *Hepacivirus* genus. Infection with HCV leads to chronic liver diseases, including cirrhosis and hepatocellular carcinoma (16). HCV is a major public health problem, infecting an estimated 170 million people worldwide (6, 16, 19). Current standard therapy for HCV-related chronic hepatitis is based on the combination of interferon (IFN) and ribavirin although virus eradication rates are limited to around 50% (7, 24, 30). Telaprevir and boceprevir were approved by the U.S. Food and Drug Administration in 2011 in combination with pegylated alpha interferon and ribavirin for the treatment of genotype 1 chronic hepatitis C (34, 35). Both agents inhibit the NS3-NS4A serine protease essential for replication of HCV (25, 36). It is important to develop more anti-HCV drugs with different modes of action to achieve greater efficacy and to avoid the emergence of drug-resistant viruses. To that end, a detailed understanding of the viral replication mechanism is needed to discover novel antiviral targets. An efficient virus culture system is indispensable for detailed analysis of HCV life cycles. In an important development, a subgenomic HCV RNA replicon system has been developed (22) to assess HCV replication in cultured cells. Furthermore, an efficient HCV culture system was established by using a JFH-1 strain virus isolated from a fulminant hepatitis patient (20, 38, 41). By transfection of *in vitro* transcribed full-length JFH-1 HCV RNA into HuH-7 cells, efficient JFH-1 RNA replication and infectious viral particle production were detected. However, this efficient virus production was not reproduced by other HCV strains, even when adaptive mutations were introduced to enhance the replication efficiency in cultured cells (29). Thus, other HCV strains that can replicate in cultured cells and produce infectious virus particles are needed. The J6CF strain is infectious to chimpanzees but does not replicate in cultured cells (26, 27, 40). We constructed chimeric replicon and virus constructs of the J6CF and JFH-1 strains to elucidate the difference in their molecular mechanisms (26, 27). We determined that the NS3 helicase and the NS5B to 3′X regions are important for the efficient replication of the JFH-1 strain and that several amino acid mutations in the C terminus of NS5B are pivotal for replication. However, we could not rescue the replication of other virus strains, such as Con1, with these mutations. This result indicates that different approaches are needed to create replication-competent virus strains in cultured cells.

In the present study, we isolated HCV cDNA, named JFH-2, from a fulminant hepatitis patient. The replication efficiency of the JFH-2 clone in the subgenomic replicon assay was lower than that of JFH-1 although the introduction of adaptive mutations enhanced JFH-2 replication. Interestingly, the full-length chimeric or wild-type JFH-2 genome with adaptive mutations could replicate and produce infectious virus particles. The virus infection efficiency was sufficient for autonomous virus propagation in cultured cells.

MATERIALS AND METHODS

Cell culture system. HuH-7, Huh-7.5.1 (a generous gift from Francis V. Chisari), and Huh7-25 cells were cultured in 5% CO_2 at 37°C in Dulbec-

Received 29 December 2011 **Accepted** 2 July 2012
Published ahead of print 11 July 2012
Address correspondence to Takaji Wakita, wakita@nih.go.jp.
* Present address: Hitoshi Takahashi, Influenza Virus Research Center, National Institute of Infectious Diseases, Musashimurayama, Tokyo, Japan; Kenichi Morikawa, Division of Gastroenterology and Hepatology, Centre Hospitalier Universitaire Vaudois, University of Lausanne, Lausanne, Switzerland; Tetsutaro Sata, Toyama Institute of Health, Toyama, Japan.

doi:10.1128/JVI.07235-11

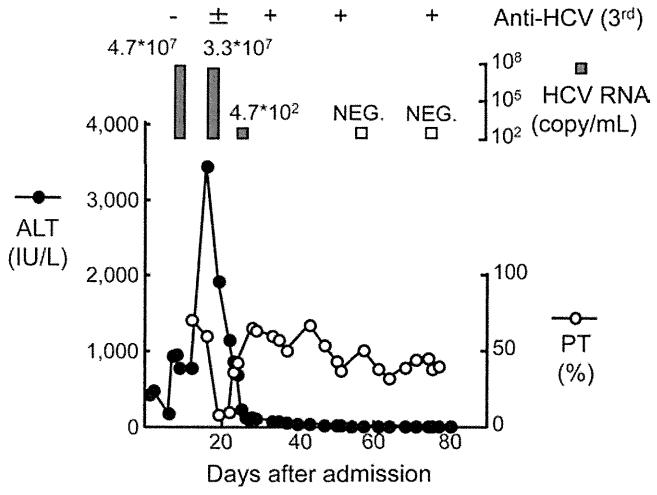

FIG 1 Clinical course of second fulminant hepatitis patient infected with JFH-2. The patient was admitted by reason of acute liver failure. Alanine aminotransferase (ALT) levels, prothrombin time (PT), HCV RNA, and anti-HCV antibodies were determined and followed in his serum.

co's modified Eagle's medium (DMEM) containing 10% fetal bovine serum (DMEM-10) (3, 41).

HCV clones. The genotype 2a clone JFH-2 was isolated from a patient with fulminant hepatitis (15). Briefly, HCV cDNA was cloned from a fulminant hepatitis patient, a 62-year-old man who had a history of coronary artery bypass surgery without blood transfusion. One year after the surgery, he developed an acute auditory disorder and received a course of betamethasone therapy. After withdrawal of betamethasone, the patient developed fulminant hepatitis as diagnosed by acute liver failure associated with stage II encephalopathy and low prothrombin time. He experienced prolonged liver failure and died after 80 days. HCV RNA was detected in his serum only during the acute phase (Fig. 1). Total RNA was extracted from serum during the acute phase, and HCV cDNA covering the entire genome was amplified by reverse transcription-PCR (RT-PCR). All amplified products were purified and then cloned into pGEM-T EASY vectors (Promega, Madison, WI). PCR products and plasmids were sequenced by using specific primer sets (Table 1), BigDye Terminator Mix, and an automated DNA sequencer (models 310 and 377; PE Biosystems, Foster City, CA). The JFH-2 subgenomic replicon (SGR) clones, pSGR-JFH2.1 and pSGR-JFH2.2 (DDBJ/EMBL/GenBank accession numbers AB690456 and AB690457, respectively), were constructed according to the method for pSGR-JFH1 construction (11). Several mutations were introduced into the pSGR-JFH2.1 replicon construct, as reported previously (11). The reporter replicon constructs, pSGR-JFH2.1/Luc and pSGR-JFH2.1/Luc, were developed by rearrangement with pSGR-JFH2.1 and pSGR-JFH2.2 (accession numbers AB690458 and AB690459, respectively) as described previously (12). pJ6/JFH1 was previously obtained from pJFH1 by replacement with the 5′ untranslated region (UTR) to the p7 region (EcoRI-BclI) of the J6CF strain (a kind gift from Jens Bukh) (3, 40). A full-length HCV cDNA was constructed by using the 5′ end to NS2 of pJ6/JFH1 and NS3 to the 3′ end of pSGR-JFH2.1, and the resulting construct was named pJ6/JFH2 (accession number AB690460). Another full-length HCV construct, pJFH2 containing the full-length JFH-2 cDNA downstream of the T7 RNA promoter sequence, was also constructed by replacing the 5′ UTR to NS2 of pJ6/JFH2 with JFH2 sequences, as described previously (accession number AB690461) (1, 37, 38).

Subgenomic replicon assay. Subgenomic replicon RNA was synthesized as reported previously (11). Synthesized replicon RNA was adjusted to 10 μg with cellular RNA isolated from untransfected HuH-7 cells and then electroporated into naive HuH-7 cells as reported previously (11). G418 (1.0 mg/ml) was added to the culture medium, and the drug-resistant colonies were fixed with buffered formalin and stained with crystal violet or cloned and expanded for further analysis. Total RNA was extracted from the cloned G418-resistant cells by using Isogen reagent (Nip-

TABLE 1 Primer list used for cloning and sequencing of JFH-2 clone

Forward primer		Reverse primer	
Name	Sequence (5′→3′)	Name	Sequence (5′→3′)
44S	CTGTGAGGAACTACTGTCTT	1323R	GGTGACCAGTTCATCATCAT
317S	GGGAGGTCTCGTAGACCGTG	1440R	GCTCCCTGCATAGAGAAGTA
844S	GGGTTAATTATGCAACAGGGAAC	2367R	CATTCCGTGGTAGAGTGCA
1141S	TGTCCGCCACGCTCTGCT	2445R	TCCACGATGTTTTGGTGGAG
1361S	CCCGAGGTCATCATAGACAT	3568R	TGTTCCGAGGAAGGACTGAG
2106S	CTGTTGTGCCCCACGGACTG	3765R	TCAGCGTTCCGCGTGACCA
2285S	AACTTCACTCGTGGGGATCG	4706R	TTGCAGTCGATCACGGAGTC
3211S	GGCACTTACATCTATGACCACCTC	5331R	GAGGTCATGACCAGCACGTG
3471S	TGGGCACCATAGTGGTGAG	5563R	CTGCAGCAAGCCTTGGATCT
3930S	TCGATTTCATCCCCGTTGAG	5970R	TTCTCGCCAGACATGATCTT
4278S	CCTATGACATCATCATATGCGATGAATGCC	6152R	AGTGAGTAGGGGCGACGTGGTTTCCTCTGG
4301S	CCTATGACATCATCATATGCGATG	6505R	CCTGCCAGGTGTTCATGCAG
4547S	AAGTGTGACGAGCTCGCGG	6605R	GCATACTCTGAGGCCGCCAC
5021S	TTTTGGGAGGCAGTTTTCAC	6897R	GTGATGTGGGGCGGATCTGTTAGCATGGAC
6383S	TGTCAAAAGGGGTACAAGGG	7648R	TCCTCCTCGGAGCAAGTAGA
6774S	TCCGGGATGAGGTCTCGTTC	8913R	GCGTACTGGATGATGTTTCC
6881S	ATTGATGTCCATGCTAACAG	3X-54R	GCGGCTCACGGACCTTTCAC
7198S	GGCTTGGGCACGGCCTGA	3X-75R	TACGGCACTCTCTGCAGTCA
7244S	ACCGCTTGTGGAATCGTGGA		
7657S	CGTGTGCTGCTCCATGTCAT		
7993S	CAGCTTGTCCGGGAGGGC		
8337S	TTTCGTATGATACCCGATGCTT		
8704S	CGCCCCTCCGGGTGACCCCCCCAGACCGGA		
9123S	CACGAACTGACGCGGGTGGC		

pon Gene, Tokyo, Japan), and the replicon RNA was quantitated by Northern blotting and real-time detection RT-PCR as reported previously (11, 37). The cDNAs of the HCV RNA replicon were synthesized and then amplified by PCR. The sequence of each replicon was determined.

Luciferase reporter replicons were analyzed as follows. Five micrograms of synthesized replicon RNA was transfected into HuH-7 cells by electroporation. Transfected cells were harvested serially at 4, 24, 48, 72, and 96 h after transfection. Luciferase activities were quantified by a Lumat LB9507 instrument (EG&G Berthold, Bad Wildbad, Germany) and a luciferase assay system (Promega). Assays were performed at least in triplicate, and the results were expressed as relative luciferase activity.

Analysis of G418-resistant cells. In RNA-transfected dishes, G418-resistant colonies were isolated by using a cloning cylinder (Asahi Techno Glass Co., Tokyo, Japan) and expanded until 80% to 90% confluence in 10-cm diameter dishes. Expanded cells were analyzed as described previously (11).

Northern blot analysis. Four micrograms of isolated RNA samples was electrophoretically separated in a 1% agarose gel containing formaldehyde and transferred to a positively charged nylon membrane (Hybond-N+; GE Healthcare UK, Ltd., Buckinghamshire, England) and immobilized by a Stratalinker UV cross-linker (Stratagene, La Jolla, CA). Hybridization was performed with a [α-^{32}P]dCTP-labeled DNA probe by using Rapid-Hyb Buffer (GE Healthcare UK, Ltd.). The NS3 to 3′X region of the JFH-1 sequence was used as a template of DNA probe synthesis with a Megaprime DNA Labeling System (GE Healthcare UK, Ltd.) (37).

Western blot analysis of HCV proteins. The protein samples were separated on a 10% polyacrylamide gel. After electrophoresis, the proteins were transferred to a polyvinylidene difluoride membrane (Immobilon; Millipore Corp., Bedford, MA) with a semidry blotting apparatus (Biocraft, Tokyo, Japan). Transferred proteins were incubated with blocking buffer containing 5% nonfat dry milk (Snow brand, Sapporo, Japan) in phosphate-buffered saline. Anti-NS3 rabbit polyclonal antibody raised against recombinant NS3 protein and horseradish peroxidase-labeled goat anti-rabbit Ig (BioSource, Camarillo, CA) were used to detect HCV NS3 protein. The signals were detected with a chemiluminescence system (ECL Plus; GE Healthcare UK, Ltd.). The quantity and quality of the loaded samples were confirmed to be similar by Coomassie brilliant blue staining of the gel.

RT-PCR and sequencing analysis. The cDNAs of HCV RNA were synthesized from total cellular RNA isolated from replicon RNA-transfected cells or from the culture medium of full-length HCV RNA-transfected cells with antisense primer in the 3′X tail region. These cDNAs were subsequently amplified with DNA polymerase (TaKaRa LA Taq; TaKaRa Bio Inc.). The sequence of each amplified DNA was determined directly as described above.

Full-length HCV RNA transfection. Full-length HCV RNA was synthesized from pJ6/JFH2, pJFH2, and the derivatives of these constructs with adaptive mutations, as described previously (13, 37, 38). Synthesized HCV RNA (10 μg) was transfected into Huh-7.5.1 or Huh7-25 cells. HCV core protein levels in the culture medium were measured by immunoassay (31). HCV RNA levels in the culture medium were quantified as described above. Infectivity of culture supernatants was determined by measuring the focus formation efficiency (13, 41). In some experiments, HCV core protein levels in the transfected cells were determined as described previously (37, 38). To examine virus secretion and infectivity after long-term culture, the transfected cells were serially passaged. Virus infection was neutralized by using mouse anti-CD81 monoclonal antibody (clone JS-81; BD Pharmingen, Franklin Lakes, NJ) and anti-HCV human IgG purified from HCV carrier serum (a gift from H. Yoshizawa and J. Tanaka, Hiroshima University).

Density gradient analysis. Culture medium derived from the transfected or infected cells was harvested for density gradient analysis. Cleared culture medium was layered onto a stepwise sucrose gradient (60% [wt/vol] to 10%) and centrifuged for 16 h in an SW41 rotor (Beckman, Palo Alto, CA) at 200,000 $\times$ *g* at 4°C. After centrifugation, 18 fractions were harvested from the bottom of the tubes. The HCV core protein, HCV RNA levels, and infectivity in each fraction were determined as described above.

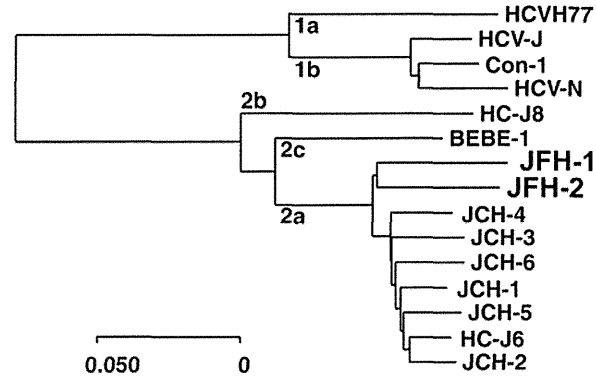

FIG 2 Phylogenetic analysis of JFH-2. Phylogenetic tree of the NS3 to NS5B amino acid sequences of HCV including the JFH-2 strain and genotype 2 strains for which the entire genome has been reported (JFH-1, accession number AB047639; HC-J6, D00944; HC-J8, D10988; and BEBE1, D50409) and representative genotype 1 strains for which the entire genome has been reported (H77, AF009606; HCV-Con1, AJ238799; HCV-J, D90208, and HCV-N, AF139594). This phylogenetic tree was drawn by using Kimura's two-parameter method.

Electron microscopy. To visualize HCV particles, we adsorbed the density gradient-purified virus samples onto carbon-coated grids for 1 min. Then, the grids were stained with 1% uranyl acetate for 1 min and examined under an H-7650 transmission electron microscope (Hitachi High-Technologies Co., Tokyo, Japan) (32). Immunogold labeling was performed with an antibody directed against E2 (AP33; a kind gift from Genentech, South San Francisco, CA) diluted 1:50 in blocking solution and secondary antibody coupled to 10-nm gold particles.

Human hepatocyte chimeric mouse experiments. Human hepatocytes were transplanted into urokinase-type plasminogen activator-transgenic SCID mice(uPA$^{+/+}$ SCID$^{+/+}$) as described previously (33). All mice received hepatocyte transplants from the same donor. Human hepatocyte chimeric mice, in which liver cells were largely (>90%) replaced with human hepatocytes, were used to reduce the potential influence by mouse-derived mRNA. Human albumin levels in the sera of mice were monitored to evaluate the replacement ratio of the human hepatocytes in the mouse liver. The mice were obtained from Phoenix Bio Co., Ltd. (Hiroshima, Japan). Four mice were divided into two groups. Each group of mice was inoculated with 1×10^6 RNA copies of either purified J6/JFH2/AS HCV particles or JFH-2 patient serum. The HCV RNA titer in inoculated mouse serum was monitored by real-time detection RT-PCR each week after inoculation.

RESULTS

HCV clone from a fulminant hepatitis patient. HCV cDNA was isolated from a fulminant hepatitis patient as described in Materials and Methods (clone JFH-2) (15). HCV RNA was detected by RT-PCR in the patient's serum during the acute phase (Fig. 1). All viral markers of the other hepatitis viruses were negative. By the phylogenetic analysis, the JFH-2 clone was clustered into genotype 2a (Fig. 2). JFH-2 exhibits 87.6%, 89.0%, and 88.9% nucleotide homology with JFH-1, J6CF, and JCH-1, respectively, and 90.6%, 91.8%, and 91.8% amino acid homology with JFH-1, J6CF, and JCH-1, respectively (Table 2). The JFH-1 strain is cell culture replication-competent, but the J6CF and JCH-1 strains are incompetent. However, the homology data for nucleotide and amino acid sequences are very similar in both the structural and nonstructural regions. We also mapped the